ORGANOMETALLICS

pubs.acs.org/Organometallics Article

Ring-Opening Polymerization of ε -Caprolactone Utilizing Aluminum Alkyl Complexes Bearing Dianionic Scorpionate Ligands

Elizabeth N. Cooper, Boris Averkiev, Victor W. Day, and Peter E. Sues*



Cite This: Organometallics 2021, 40, 3185-3200



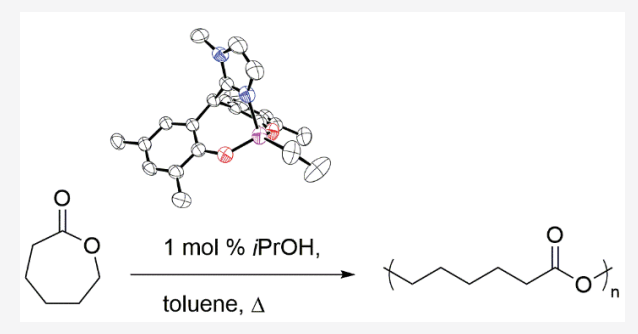
ACCESS

Metrics & More

Article Recommendations

Supporting Information

ABSTRACT: A series of eight scorpionate ligands $(Ar)_2CHR$ (1–4) were synthesized and coordinated to aluminum to produce $Al(CH_2CH_3)((Ar)_2CHR)$ (5–8), where $R = CH_2OCH_3$ (1 or 5), $CH_2N(CH_3)_2$ (2 or 6), imidazole (3 or 7), or *N*-methylimidazole (4 or 8), and Ar = 2,4-dimethylphenol (a) or 2-tert-butyl-4-methylphenol (b). The bisphenol compounds were generated using a Friedel–Crafts alkylation reaction starting with commercially available reagents. The scorpionate species were subsequently combined with triethylaluminum in order to probe the coordination geometries of 1–4. The resulting complexes 5–8 displayed distorted tetrahedral structures with the bisphenolate ligands acting as tridentate donors. The only exception was 5a, which formed



phenolate bridged dimers in the solid state. Additionally, complexes 5-8 were found to be active catalysts for the ring-opening polymerization of ε -caprolactone. The aluminum alkyl species affected this transformation both with and without the use of an alcohol co-catalyst, but higher activities and cleaner activations were seen when 1 equiv of iPrOH was employed. The less sterically hindered complexes with more weakly bound hemilabile "tails" showed the highest activities, with nearly 100% conversion after 1 h at 50 °C, and a catalyst loading of 1 mol %.

■ INTRODUCTION

Petroleum-based polymers such as polyethylene and polypropylene have found widespread commercial use due to their chemical stability and physical durability. As such, they are produced on million tonne (Mt) scales globally every year, with over 359 Mt produced in 2018. 1,2 The desirable properties of petroleum-based plastics, however, causes problems when it comes to their disposal. Polyethylene and polypropylene polymers are not biodegradable and persist in natural environments. The most dramatic example of this is the Great Pacific Garbage Patch, which is estimated to have a surface area of 1.6 million square kilometers, or roughly twice the size of Texas.³⁻⁶ In addition, petroleum feedstocks are rapidly depleting, making the use of petroleum-based plastics unsustainable in the long term. The development of biodegradable polymers, therefore, is highly desirable and has received increasing attention in recent years. 10-12 Polyesters such as polylactide and polycaprolactone (PCL), which are generated through the ring-opening polymerization (ROP) of lactide and ε -caprolactone (ε -CL), respectively, are particularly promising because of their favorable degradation properties, and renewable feedstocks. 12,13

Metal-mediated processes have been a specific area of interest for the ROP of cyclic esters as well-defined biodegradable polymers with controlled chain lengths are produced. Aluminum-based systems are especially attractive due to the large abundance of the metal, its low cost, and

its high Lewis acidity. ^{14,16–18} When developing catalytic systems, though, the ancillary ligands surrounding the aluminum center play a key role in determining the reactivity and selectivity of the catalyst. Over the past several decades, aluminum complexes bearing bidentate, ^{19–31} tridentate, ^{32–37} and tetradentate ^{35,38,39} ligands have been explored in the literature, a selection of which are shown in Figure 1. ^{15,40–45} Notably, aluminum alkyl complexes supported by salen ^{46–51} or salan ^{52–54} ligands have seen particular success in this field. These species form five-coordinate pre-catalysts that can polymerize cyclic esters with narrow PDIs after being activated with benzyl alcohol.

Scorpionate ligands, on the other hand, were first developed in the late 1960s by Trofimenko, and include species like tris(pyrazolyl)borate fall and tris(pyrazolyl)methane (Figure 2). The defining features of these ligands are a fac coordination geometry and the ability to interchange between tridentate and bidentate binding modes. This hemilability can lead to higher reactivity levels over other tridentate ligands,

Received: July 3, 2021

Published: September 9, 2021





Figure 1. Examples of aluminum ROP catalysts bearing bidentate (left), tridentate (middle), and tetradentate (right) ligands.

Figure 2. General structures for tris(pyrazolyl)borate (left) and tris(pyrazolyl)methane (right) scorpionate ligands.

such as pincer ligands, which tend to form very stable complexes. 60,61 Moreover, scorpionate ligands are extremely versatile in that their bonding strengths, electronic parameters, and steric encumbrance can be readily tuned. Since their development, complexes incorporating these types of ligands have been widely studied for medical purposes, ⁶² catalysis, ⁶³ as well as other applications. 62,64,65 Surprisingly, despite their versatility, to the best of our knowledge, only a handful of scorpionate ligands have been explored on aluminum centers. 66-68 Martinez et al. investigated a family of aluminum scorpionate complexes for the catalytic synthesis of cyclic carbonates from epoxides and carbon dioxide. $^{66,69-71}$ Additionally, aluminum scorpionate complexes have been utilized by the Otero group, and others, to affect the ROP of lactide and ε -CL. ^{67,71–75} By increasing the steric bulk of the tridentate ligands, more control over polymerization was seen and products with narrower PDIs were generated.⁷⁴ It would therefore be of great interest to further explore this underutilized ligand class in the context of aluminum catalyzed ROP of cyclic esters.

Herein, the straightforward synthesis of dianionic scorpionate ligands with two phenolate donors and a third hemilabile "tail" is reported, as is their characterization. In addition, the first metal complexes bearing these tridentate ligands, tetrahedral aluminum alkyl compounds, are discussed and the coordination geometry of the ligands is investigated. Lastly,

the catalytic activity of the aluminum species for the ROP of ε -CL is explored in relation to the steric demands of the ligands and the nature of the hemilabile "tail". With respect to nomenclature, throughout this paper, the scorpionate ligands will be named according to their neutral donor functionality (1 for methoxy; 2 for dimethylamino; 3 for imidazolyl; 4 for N-methylimidazolyl) and the substituents ortho to the phenol groups (a for methyl; b for tert-butyl), while the aluminum complexes will be named according to the bound scorpionate ligand (5a,b for 1a,b; 6a,b for 2a,b; 7a,b for 3a,b; 8a,b for 4a,b).

■ RESULTS AND DISCUSSION

Synthesis and Characterization of Scorpionate Ligands 1–4. Compounds 1–4 were synthesized using a Friedel–Crafts alkylation reaction under acidic conditions. Two equivalents of phenol (2,4-dimethylphenol for a, or 2-tert-butyl-4-methylphenol for b) and 1 equiv of protected aldehyde (methoxyacetaldehyde diethylacetal for 1, or dimethylaminoacetaldehyde diethylacetal for 2) or aldehyde (2-imidazolecar-boxaldehyde for 3, or 1-methyl-2-imidazolecarboxaldehyde for 4) were combined in an acetic acid/sulfuric acid mixture to yield 1–4 as white solids in poor to moderate yields (24–50%, Scheme 1). For ease of isolation, the dimethylamino variants were first isolated as hydrochloride salts, 2a·HCl and 2b·HCl, and then neutralized with base to give the desired neutral species, 2a and 2b.

The ¹H NMR spectra of compounds 1–4 exhibited several diagnostic peaks that confirmed the presence of the proposed structures (see Supporting Information for ¹H NMR spectra of 1–4). All eight scorpionate ligands showed the disappearance of the hydrogen *ortho* to the phenol moiety, as well as the loss of its coupling to the adjacent *meta*-hydrogen. Moreover, the appearance of a triplet between 4.5 and 5.1 ppm (CH-CH₂) in 1a,b and 2a,b, as well as a doublet between 3.0 and 3.8 ppm (CH-CH₂), indicated that the methoxy and dimethylamino "tails" had been incorporated. For 3a,b and 4a,b, on the other hand, the appearance of a singlet between 5.7 and 6.0 ppm

Scheme 1. General Synthetic Procedure for Scorpionate Ligands 1-4

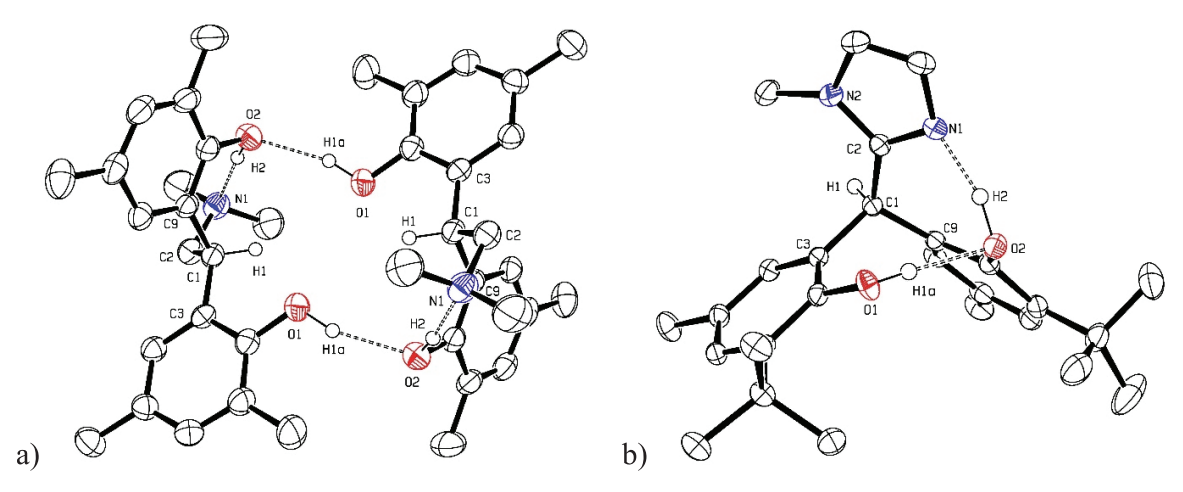


Figure 3. ORTEP3 representation (thermal ellipsoids at 50% probability) and atom numbering for: (a) 2a, most of the hydrogens are omitted for clarity; and (b) 4b, most of the hydrogens are omitted for clarity.

(tertiary carbon) revealed that the imidazolyl and *N*-methylimidazolyl functionalities had been installed.

In addition to NMR experiments, compounds 2a and 4b were characterized in the solid state utilizing single-crystal X-ray diffraction (Figure 3). In both tridentate ligands, the central tertiary carbon linking the two phenol moieties and the "tail" functionality (dimethylamino in 2a; N-methylimidazolyl in 4b) adopts a distorted tetrahedral geometry (for notable bond lengths and angles, see Table 1). The C-C-C bond

Table 1. Selected Bond Lengths (Å) and Angles (deg) for 2a and 4b

	2a	4b
	bond ler	ngths (Å)
C(1)-C(2)	1.542(9)	1.513(4)
C(1)-C(3)	1.515(9)	1.542(4)
C(1)-C(9)	1.537(6)	1.541(4)
C(1)-H(1)	0.99(6)	0.99
H(1a)···O(2)	1.94	1.82
H(2)···N(1)	1.67	1.56
	bond ang	gles (deg)
C(2)-C(1)-C(3)	111.8(6)	114.3(4)
C(2)-C(1)-C(9)	111.0(6)	117.8
C(3)-C(1)-C(9)	112.9(6)	110.8
C(2)-C(1)-H(1)	108.0(4)	104.3
C(3)-C(1)-H(1)	105.8(4)	104.1
C(9)-C(1)-H(1)	106.8(3)	103.8
O(1)-(H1a)-O(2)	162.3	175.0
O(2)-H(2)-N(1)	163.4	162.8

angles are all larger than the optimal 109.5° angle for a perfect tetrahedron, with values of $112.9(6)^{\circ}$, $111.0(6)^{\circ}$, and $111.8(6)^{\circ}$ in 2a, as well as $110.8(2)^{\circ}$, $117.8(4)^{\circ}$, and $114.3(4)^{\circ}$ in 4b, for C(3)-C(1)-C(9), C(2)-C(1)-C(9), and C(2)-C(1)-C(3), respectively. This is likely due to steric strain between the three large substituents. In order to compensate for these larger bond angles, the C-C-H bond angles are all compressed below 109.5° . Interestingly, while the largest C-C-C bond angle for the tertiary carbon in 2a, $112.9(6)^{\circ}$, is between the two largest substituents (the phenol groups), in 4b, this is actually the smallest C-C-C bond angle for the tertiary carbon, $110.8(2)^{\circ}$. This disparity can be

attributed to the difference in hydrogen bonding exhibited by the two scorpionate species (Figure 3). In 2a, both inter- and intramolecular hydrogen bonding occurs: one hydroxyl group is hydrogen bonded to the dimethylamino moiety (H(2)... N(1), 1.67 Å, intramolecular), whereas the other hydroxyl group is hydrogen bonded to the oxygen of an adjacent molecule (H(1a)···O(2), 1.94 Å, intermolecular). As such, in the solid state, 2a forms hydrogen bonded dimers where the ligand donors (O(1), O(2), and N(1)) are oriented in roughly the same direction as the tertiary carbon's C(1)-H(1) bond. For 4b, in contrast, only intramolecular hydrogen bonding can be seen: one hydroxyl functionality is hydrogen bonded to the imidazole nitrogen $(H(2) \cdots N(1), 1.56 \text{ Å})$, while the other hydroxyl is hydrogen bonded to the oxygen atom of the adjacent phenol (H(1a)···O(2), 1.82 Å). It is believed that the interaction between the two hydroxyl groups in 4b compresses the C(3)-C(1)-C(9) bond angle, which is why it is smaller than the other C-C-C bond angles discussed above. Additionally, it is hypothesized that the tert-butyl groups in 4b prevent hydrogen bonded dimers from forming. For 2a, the methyl groups ortho to the phenol groups point toward each other in adjacent molecules and increased steric bulk in these positions could disrupt intermolecular hydrogen bonding.

The modular nature of the synthetic procedure outlined above (Scheme 1) is particularly exciting as it represents a general route for accessing a wide variety of scorpionate ligands using commercially available reagents where the steric and electronic properties of the targeted species can be readily varied. A wide range of "tail" groups were tolerated, including imidazolyl, amino, and ethereal functionalities, and it is hypothesized many other groups will be tolerated as well. As such, the donating ability of the hemilabile donor can be easily tuned to increase or decrease binding strength. Moreover, the scope of this reaction was not limited to free aldehydes as protected aldehydes could also be utilized. A limitation of this procedure, however, is that a strong acid is needed to facilitate the Friedel—Crafts alkylation, which precludes the used of acid-sensitive functionalities.

With respect to the phenol starting materials, reagents with methyl and *tert*-butyl substituents *ortho* to the hydroxyl groups were successfully utilized. This suggested that the formation of the tridentate compounds was relatively insensitive to steric encumbrance in those positions and that a wide variety of alkyl

Scheme 2. General Synthetic Procedure for Accessing Scorpionate Complexes 5-8

Scheme 3. Formation of 8b via a Dialkyl Intermediate

substituents would be tolerated. This provides a convenient avenue for varying the bulkiness of the targeted scorpionate compounds by simply changing the nature of the phenol starting materials. It should be noted, though, that initial attempts to utilize phenols with electron rich aryl groups *ortho* to the hydroxyl moieties were unsuccessful. It is likely that the increased conjugation decreased the nucleophilicity of the phenol ring, which prevented the reaction from proceeding.

Synthesis and Characterization of Aluminum Complexes 5–8. In order to probe the binding modes of compounds 1–4, the scorpionate ligands were combined with triethylaluminum and the resulting complexes were characterized. The bisphenol species were cleanly deprotonated at room temperature in benzene, leading to the evolution of ethane gas and the formation of four-coordinate aluminum complexes, 5–8, which could be isolated as white solids in poor to good yields (27–83%, Scheme 2). The only exception was 4b, which initially formed an asymmetric, monodeprotonated aluminum intermediate with two ethyl groups and only one phenolate donor bound to the metal center, as determined by ¹H NMR spectroscopy (Scheme 3). Heating this species at 70 °C, however, yielded the desired product, 8b.

The 1 H NMR spectra of compounds 5–8 (except 5a, which will be addressed separately below) all showed characteristic peaks that were shifted from the free ligand forms (see Supporting Information for 1 H NMR spectra of 5–8). Additionally, the absence of the hydroxyl signals between 10 and 11 ppm was notable, as was the presence of ethyl peaks: a triplet between 1.4 and 1.7 ppm (Al-CH₂CH₃), as well as a quartet between 0.3 and 0.8 ppm (Al-CH₂CH₃).

In addition to NMR spectroscopy, complexes 5a, 6a,b, 7a,b, and 8a were characterized in the solid state utilizing single-crystal X-ray diffraction (Figure 4). In all six structures, the aluminum centers adopted distorted tetrahedral coordination geometries. Unlike the other five compounds, however, 5a

formed dimeric species where the ethereal "tail" of the scorpionate ligand was not bound to aluminum. Instead, a phenoxide donor bridged between two metal centers, generating a diamond shaped core with bond angles of 99.78(9)° and 80.22(9)° for Al(1)-O(1)-Al(1)* and O(1)- $Al(1)-O(1)^*$, respectively, as well as an $Al(1)-Al(1)^*$ distance of 2.819(2) Å (* denotes an atom belonging to the other half of the dimer). Additionally, the O(1)-Al(1)-O(2)angle was slightly compressed, 109.0(1)°, likely because of the bidentate binding mode of 1a. All of the O-Al-C bond angles, in contrast, were significantly larger than the optimal 109.5° angle for a perfect tetrahedron: $112.2(2)^{\circ}$, $118.9(2)^{\circ}$, and 121.2(2)° for O(1)-Al(1)-C(1E), C(1E)-Al(1)- $O(1)^*$, and O(2)-Al(1)-C(1E), respectively. It is hypothesized that the weaker binding ability of the methoxy group, as well as the sterically unencumbered methyl substituents ortho to the oxygen donors, allowed this structure to form. Interestingly, the asymmetric binding mode of the bisphenolate ligand in 5a is similar to that of the protonated ligand 2a in the solid state, in that the oxygen donors, O(1), O(2), and O(3), are all oriented in roughly the same direction as the tertiary carbon's C-H bond, C(1)-H(1). As such, the C-C-H and C-C-C bond angles for the tertiary carbon in 5a are similar to those seen in 2a (for notable bond lengths and angles, see Table 2).

While **5a** is dimeric in the solid state, in solution, this structure appears to be less favored. The ¹H NMR spectrum showed multiple compounds in solution, with the monomeric complex as the major species. It is believed that the hemilabile "tail" is bound to the metal in this monomeric structure due to the symmetric environment of the scorpionate ligand, in contrast to the asymmetric binding mode seen in the crystal structure. Additionally, similar chemical shifts were seen for this major species and **5b**; both complexes displayed characteristic peaks that were shifted from the free ligand

 Organometallics
 pubs.acs.org/Organometallics
 Article

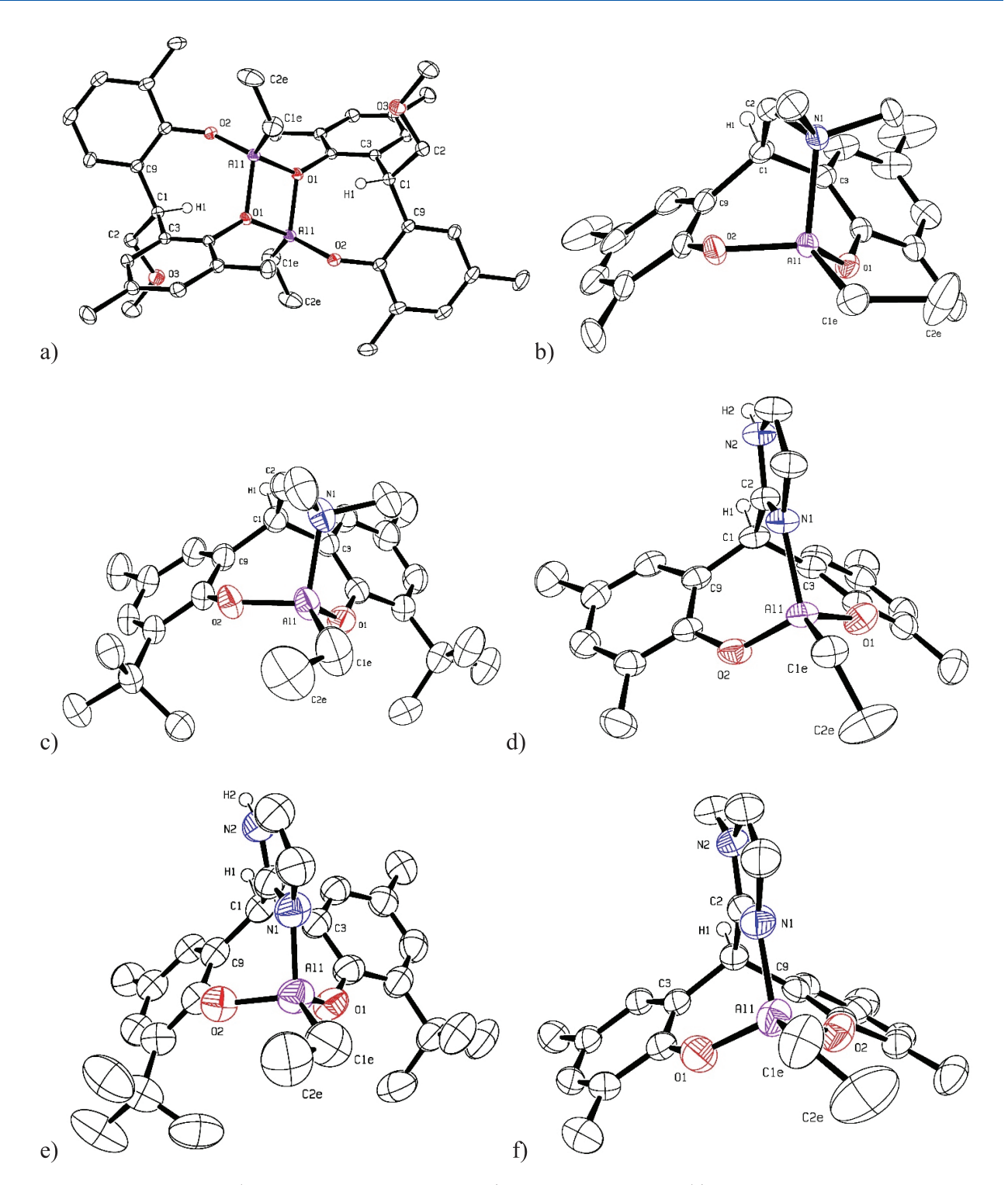


Figure 4. ORTEP3 representation (thermal ellipsoids at 50% probability) and atom numbering for: (a) 5a, the solvent and most of the hydrogens are omitted for clarity; (b) 6a, the solvent and most of the hydrogens are omitted for clarity; (c) 6b, most of the hydrogens are omitted for clarity; (d) 7a, the solvent and most of the hydrogens are omitted for clarity; (e) 7b, the solvent, one of the aluminum complexes (two complexes are present in the asymmetric unit), and most of the hydrogens are omitted for clarity; and (f) 8a, the solvent and most of the hydrogens are omitted for clarity.

forms including an overlapping doublet and triplet between 3.67 and 3.72 ppm (for CH-CH₂ and CH-CH₂ in the tail functionality). The other unidentified compounds in solution are hypothesized to be dimers, trimers, and other clusters, but

due to their relatively low concentrations, full characterization was not possible. It should also be noted that identical ¹H NMR spectra were obtained using single crystals suitable for X-ray diffraction and amorphous powders obtained through

Table 2. Selected Bond Lengths (Å) and Angles (deg) for $5a^a$

	5a
	bond lengths (Å)
Al(1)-Al(1)	2.819(2)
Al(1)-O(1)	1.854(2)
$Al(1) - O(1)^{b}$	1.832(2)
Al(1)-O(2)	1.713(2)
Al(1)-C(1E)	1.941(4)
	bond angles (deg)
Al(1)-O(1)-Al(1)	99.78(9)
$O(1)-Al(1)-O(1)^{c}$	80.22(9)
O(1)-Al(1)-O(2)	109.0(1)
$O(1)-Al(1)-O(2)^{c}$	108.0(1)
O(1)-Al(1)-C(1E)	112.2(2)
$O(1)-Al(1)-C(1E)^{c}$	118.9(2)
O(2)-Al(1)-C(1E)	121.2(2)
C(2)-C(1)-C(3)	111.0(2)
C(2)-C(1)-C(9)	112.2(2)
C(3)-C(1)-C(9)	111.7(2)
C(2)-C(1)-H(1)	107.2
C(3)-C(1)-H(1)	107.2
C(9)-C(1)-H(1)	107.2

"The asymmetric unit of 5a only includes half of the dimeric species, and as such, the labels for both halves of the dimer are identical. "This bond length describes the Al-O bond distance to the O(1) oxygen donor from the half of the dimer not displayed in the asymmetric unit. "These bond angles describe the O-Al-O or O-Al-C bond angles with the O(1) oxygen donor from the half of the dimer not displayed in the asymmetric unit.

precipitation. This suggests that the dimers seen in the solid state break apart in solution and form the monomeric complex, as well as other bridging species. The ¹H NMR peaks were all fairly sharp, however, which indicated that the aluminum compounds in solution were either not fluxional on the NMR time scale or exchanging very quickly. If the lack of peak broadening was due to fast exchange on the NMR time scale, then it would be expected that the average of all of the species in solution would be seen. Instead, what was found was a clear

major product (the monomeric complex) that looked nearly identical to its *tert*-butyl analogue **5b**, along with some minor species in the baseline. Over the course of several days, though, the peaks associated with the monomeric aluminum complex decreased in intensity, whereas the peaks associated with the other aluminum species grew in intensity. As the protonated ligand was not seen, it is believed that this did not represent complex decomposition through protonation, but slow conversion of the monomeric complex into various bridging species in solution. This is likely due the lability of the methoxy group, as well as the sterically unencumbered methyl substituents *ortho* to the phenolate donors. Analogous behavior was not seen for **5b**, which we attribute to the bulkiness of the *tert*-butyl groups preventing bridging of the phenolate donors.

In order to further probe the behavior of 5a in solution, variable temperature ¹H NMR studies were carried out (see Figure S20 in the Supporting Information). As 5a was heated, the concentration of the monomeric species decreased, whereas the concentrations of the other species in solution grew (much like they did at room temperature over several days). As the ¹H NMR peaks remained fairly sharp while 5a was heated, interconversion between the various species in solution either did not occur or was slow on the NMR time scale. Additionally, it can be concluded that, at elevated temperatures, the monomeric form of 5a becomes less and less favored in comparison to the other aluminum compounds in solution. It is possible that, when 5a is first dissolved in solution, a kinetic distribution of products forms, which then approaches an equilibrium distribution slowly over time at room temperature, or more rapidly when heated.

In contrast to 5a, the crystal structures of complexes 6a, 6b, 7a, 7b, and 8a were all monomeric in nature, with the scorpionate ligand adopting a tridentate binding mode (Figure 4). The Al(1)-N(1) bond distances were 1.981(6), 1.967(4), 1.909(3), 1.923(9), and 1.909(9) Å for 6a, 6b, 7a, 7b, and 8a, respectively, which followed expected trends. The stronger imidazole donors formed shorter bonds with the metal in comparison to the weaker dimethylamino donors. When considering the coordination geometry about the aluminum center, the O(1)-Al(1)-N(1) and O(2)-Al(1)-N(1) bond

Table 3. Selected Bond Lengths (Å) and Angles (deg) for 6a,b, 7a,b, and 8a

	6a	6b	7a	7b	8a
			bond lengths (Å)		
Al(1)-N(1)	1.981(6)	1.967(4)	1.909(3)	1.923(9)	1.909(9)
Al(1) - O(1)	1.738(6)	1.726(4)	1.734(3)	1.726(9)	1.730(6)
Al(1) - O(2)	1.735(6)	1.725(3)	1.750(3)	1.766(9)	1.732(6)
Al(1)-C(1E)	1.996(9)	1.947(4)	1.942(4)	1.92(1)	1.95(1)
			bond angles (deg)		
O(1)-Al(1)-N(1)	103.7(3)	102.2(2)	100.3(2)	103.2(4)	101.5(4)
O(2)-Al(1)-N(1)	98.6(3)	98.6(2)	104.5(2)	95.3(4)	99.8(6)
O(1)-Al(1)-O(2)	111.7(3)	110.4(2)	102.7(2)	106.4(4)	109.5(4)
N(1)-Al(1)-C(1E)	113.5(3)	112.8(3)	114.6(2)	116.3(6)	115.0(5)
O(1)-Al(1)-C(1E)	112.0(3)	116.7(3)	116.3(2)	116.3(5)	115.1(5)
O(2)-Al(1)-C(1E)	115.9(3)	114.1(3)	116.3(2)	116.7(5)	114.1(4)
C(2)-C(1)-C(3)	116.9(6)	116.6(4)	115.3(3)	110.1(6)	115.4(6)
C(2)-C(1)-C(9)	114.6(6)	115.5(3)	111.9(3)	119.3(9)	115.1(6)
C(3)-C(1)-C(9)	114.4(6)	114.8(3)	116.5(3)	113.4(6)	113.8(6)
C(2)-C(1)-H(1)	102.7	102.2	103.7	104.0	103.4
C(3)-C(1)-H(1)	102.7	102.2	103.7	104.0	103.4
C(9)-C(1)-H(1)	102.7	102.2	103.7	104.0	103.5

angles were both significantly compressed (likely due to the tridentate binding mode of the scorpionate ligands), whereas the O(1)-Al(1)-O(2) bond angle was much more open (see Table 3). The only exceptions were 7a and 7b, which had relatively smaller O(1)-Al(1)-O(2) bond angles of $102.7(2)^{\circ}$ and 106.4(4)°, respectively. It is not entirely clear why 7a and 7b were such outliers, but this could be due to crystal packing effects, as well as intermolecular hydrogen bonding between the imidazole hydrogen and one of the phenolate donors $(H(2)\cdots O(2))$ bond distances of 2.139 and 2.011 Å for 7a and 7b, respectively). In order to compensate for these smaller bond angles, the N(1)-Al(1)-C(1E), O(1)-Al(1)-C(1E), and O(2)-Al(1)-C(1E) bond angles were all larger than 109.5°. Notably, the coordination mode of the bisphenolate ligands in 6a, 6b, 7a, 7b, and 8a is somewhat similar to that of the protonated ligand 4b in the solid state, in that the oxygen and nitrogen donors, O(1), O(2), and N(1), are all oriented in the opposite direction of the tertiary carbon's C-H bond, C(1)-H(1). As such, the C-C-H and C-C-C bond angles for the tertiary carbon in 6a, 6b, 7a, 7b, and 8a are fairly similar to those seen in 4b (for notable bond lengths and angles, see Table 3). Once again, 7a and 7b were prominent outliers in that one of the C(2)-C(1)-C(9) and C(2)-C(1)-C(3)bond angles was compressed, whereas the other was significantly larger. It is hypothesized that this difference can be attributed to crystal packing effects, as well as intermolecular hydrogen bonding.

ROP of ε -CL. Previously, four- and five-coordinate aluminum alkyl complexes have been used to affect the polymerization of cyclic esters in the presence of a co-catalyst, usually benzyl alcohol or *iso*-propanol (BnOH or *i*PrOH). To the best of our knowledge, though, very few aluminum alkyl species are catalytically active for these types of transformations without the use of an alcohol activator. With complexes 5–8 in hand, their activity for the ROP ε -CL was explored under various conditions (Scheme 4). According to the standards for ε -CL ROP established by Redshaw et al., these scorpionate complexes displayed moderate to good catalytic efficiencies.

Scheme 4. ROP of ε -Caprolactone Utilizing Aluminum Alkyl Complexes

Initial catalytic studies were performed using **6a**, as the dimethylamino complex was anticipated to display intermediate activity between **5**, with weakly bound ethereal groups, and 7–8, with strongly bound imidazole functionalities. A catalyst to substrate ratio, [Al]:[ε -CL], of 1:100 was used, and reactions were allowed to proceed for 1 h. In particular, the effects of temperature and the type of alcohol activator utilized were investigated (Table 4). In the absence of a co-catalyst, little to no polymerization was observed at room temperature and at 50 °C, as expected. If, however, the temperature was increased to 110 °C in toluene, near complete polymerization was observed after 1 h. When examining the very large molecular weight ($M_{\rm n}$) of the product formed under these conditions, it is clear that only a small fraction of the aluminum

catalyst was active. It is hypothesized that the high temperatures were needed to overcome the large kinetic barrier associated with a 1,2-migratory insertion of an alkyl group into an ester carbonyl functionality. Once this step was completed, however, a significantly more active aluminum-alkoxide intermediate was formed, which rapidly performed ROP (Figure 5). This mechanism is supported by the ¹H NMR spectra of the resulting PCL polymers, which contained ethyl end groups (see Figure S22 in the Supporting Information).

When an alcohol co-catalyst was utilized, the catalytic activity of **6a** increased greatly. This was evident from the 35% and 46% conversions observed at room temperature when activating the alkyl species with 1 equiv of EtOH or iPrOH, respectively. At higher temperatures of 50 °C, on the other hand, the ROP reactions proceeded to completion, with 97% and 98% conversions for EtOH and iPrOH, respectively. Interestingly, the less sterically hindered and more acidic EtOH co-catalyst gave products with higher molecular weights than iPrOH (theoretical $M_n = 11414$ g/mol for a polymer with 100 monomer subunits). This suggested that EtOH may have caused partial decomposition of the aluminum alkyl precatalyst. This hypothesis was further supported when 6a was pre-activated with alcohol prior to ε -CL addition. For *i*PrOH, very similar results were seen with and without pre-activation, but for EtOH, pre-activation gave increased polymer molecular weights, a higher polydispersity index (PDI), and lower catalytic conversions (likely due to increased amounts of precatalyst decomposition before substrate addition). It was also found that, if more than 1 equiv of iPrOH was utilized as a cocatalyst, the excess alcohol acted as a chain transfer agent and very short oligomers were formed with a higher PDI. The lower PDIs seen with EtOH in general, however, indicated that the smaller alcohol more uniformly activated 6a as compared to iPrOH. This can likely be attributed to the increased steric hindrance of the larger alcohol slowing down catalyst activation.

Once ROP conditions were optimized with 6a, the catalytic activities of all the aluminum scorpionate complexes were explored (for selected data, see Table 5; for the complete set of data, see Table S1 in the Supporting Information). When no co-catalyst was used, the results seen for 5-8 were similar to those obtained with 6a, as discussed above. In general, no polymerization was observed at room temperature or at 50 °C, but once temperatures reached 110 °C, nearly full conversion was achieved over a 1 h period. There were two notable outliers to this trend, however: 5b, which was unusually active, and 6b, which was unusually inactive. For 5b, 62% conversion was observed at 50 °C, whereas, for 6b, only 49% conversion was seen at 110 °C. The reasons for these discrepancies are currently unclear, but the weak donating ability of the hemilabile "tail" in 5b could lead to increased catalytic activity for this species. It might be expected that 5a should also exhibit increased catalytic activity, but variable temperature ¹H NMR studies showed that the concentration of the monomeric complex in solution decreased at higher temperatures, whereas the concentrations of the other species in solution grew (hypothesized to be dimers, trimers, and other clusters; see Figure S20 in the Supporting Information). It is possible that these bridging species are less active catalysts for the ROP of ε -CL (or completely inactive), which would explain the lower activities seen for **5a**. In fact, even with the addition of *i*PrOH, **5a** showed lower activity than initially anticipated based on the binding strength of the ethereal "tail" (see below). 6b, on the

Table 4. ROP of ε -Caprolactone Using $6a^a$

catalyst	[Al]:[ROH]:[ε -CL]	ROH	temp (°C)	conv (%) ^b	$M_{\rm n}~({\rm g/mol})^c$	$M_{\rm n} (g/{\rm mol})^d$	$M_{\rm w}/M_{\rm n}$
6a	1:0:100	N/A	rt	1	N/A	N/A	N/A
6a	1:0:100	N/A	50	7	N/A	N/A	N/A
6a	1:0:100	N/A	110	99	N/A	109455	1.98
6a	1:1:100	EtOH	rt	35	5220	5547	1.18
6a	1:1:100	EtOH	50	97	14199	16931	1.28
6a ^e	1:1:100	EtOH	50	89	14542	18063	1.36
6a	1:1:100	<i>i</i> PrOH	rt	46	6262	7860	1.35
6a	1:1:100	<i>i</i> PrOH	50	98	11817	16038	1.35
6a ^e	1:1:100	<i>i</i> PrOH	50	99	12330	16550	1.41
6a ^e	1:10:100	<i>i</i> PrOH	50	83	1658	1863	1.51

^aConditions: Toluene, 1 M ε-CL, 1 h. All entries are the average of multiple runs with a standard deviation \leq 2.5%. ^bConversions determined by ¹H NMR spectroscopy following established procedures. ^{81,82} ^cMolecular weights determined by ¹H NMR spectroscopy following established procedures. For the high molecular weight PCL polymers generated in the absence of co-catalyst, reliable integrations for the ethyl end groups could not be obtained due to their relatively small size in comparison to the monomer subunits. ^{81,82} ^dMolecular weights determined by GPC/SEC. ^eThe alcohol was added to the aluminum species and stirred for 5 min prior to addition of ε-CL in order to pre-activate the catalyst.

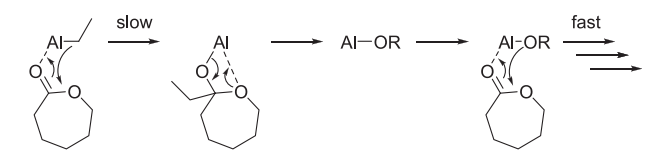


Figure 5. Proposed slow activation by aluminum-alkyl complexes, followed by rapid ROP of ε -CL by alkoxide intermediates.

other hand, is the most sterically hindered complex of the scorpionate series, which could explain its poor catalytic activity under these conditions. Moreover, all of the products generated under these conditions displayed very large molecular weights, suggesting that only a small amount of the aluminum catalyst was active in solution. In particular, 5a, 5b, and 6b gave the largest polymers, with molecular weights between 109 455 and 137 815. For 7–8, on the other hand, smaller polymers were generated with slightly reduced

Table 5. Selected Data for the ROP of ε -Caprolactone Using 5–8^a

			_			
catalyst	ROH	temp (°C)	conv (%) ^b	$M_{\rm n} (g/{\rm mol})^c$	$M_{\rm n} (g/{\rm mol})^d$	$M_{ m w}/M_{ m n}$
5a	N/A	110	98	N/A	137815	1.63
5a	iPrOH	50	18	N/A	N/A	N/A
5a	iPrOH	110	99	10618	21091	1.31
5b	N/A	50	62	N/A	52048	1.40
5b	N/A	110	>99	N/A	109643	2.35
5b	iPrOH	rt	16	N/A	N/A	N/A
5b	iPrOH	50	96	9305	17733	1.11
5b	iPrOH	110	98	8621	14618	1.75
6a	N/A	110	99	N/A	109455	1.98
6a	iPrOH	rt	46	6262	7860	1.35
6a	iPrOH	50	98	11817	16038	1.35
6a	iPrOH	110	94	11132	15613	1.72
6b	N/A	110	49	N/A	27038	1.72
6b	iPrOH	110	98	11246	14520	1.84
7a	N/A	50	14	N/A	N/A	N/A
7a	N/A	110	99	N/A	34386	1.86
7a	iPrOH	50	48	4854	6009	1.21
7a	iPrOH	110	96	11931	13462	1.77
7b	N/A	110	98	N/A	39336	1.78
7b	iPrOH	50	32	3998	4522	1.30
7b	iPrOH	110	99	10732	15453	1.72
8a	N/A	110	99	N/A	37965	1.82
8a	iPrOH	50	69	7669	11138	1.14
8a	iPrOH	110	95	10390	11891	1.73
8b	N/A	110	95	N/A	43485	1.77
8b	iPrOH	110	98	13814	15307	1.80

^aConditions: Toluene, [Al]:[iPrOH]:[ϵ -CL] = 1:1:100 or 1:0:100, 1 M ϵ -CL, 1 h. All entries are the average of multiple runs with a standard deviation ≤ 2.5% ^bConversions determined by ¹H NMR spectroscopy following established procedures. For the high molecular weight PCL polymers generated in the absence of co-catalyst, reliable integrations for the ethyl end groups could not be obtained due to their relatively small size in comparison to the monomer subunits. ^{81,82} ^cMolecular weights determined by ¹H NMR spectroscopy following established procedures. ^{81,82} ^dMolecular weights determined by GPC/SEC.

Figure 6. Proposed mechanism for the ROP of ε -CL using 5–8.

molecular weights seen for 7a and 8a. With respect to PDIs, values between 1.63 and 2.35 were observed. Interestingly, 5a had the lowest PDI, suggesting that the small percentage of catalytically active species was more uniformly activated, whereas 5b gave the highest value of 2.35. For all other catalysts, there was minimal change in the PDI when no co-catalyst was used.

Once again, very similar to the results obtained with 6a, the use of iPrOH as a co-catalyst greatly increased the catalytic efficiency of 5-8. In addition, when considering the molecular weights of the products, the addition of alcohol led to cleaner activation of the aluminum alkyl species, and generation of polymer chains closer to 100 monomer subunits long. When considering the general trends seen for 5-8, the less sterically hindered complexes with methyl substituents ortho to the phenolate donors were more active at lower temperatures when compared to the species with tert-butyl groups in these positions. This could be attributed to more facile binding of ε -CL by the less bulky catalysts, but more studies are needed. In addition, the aluminum complexes with more labile "tail" functionalities generally showed higher activities at lower temperatures. This suggests that de-coordination of one of the scorpionate ligand arms is necessary to allow catalysis to

proceed. A major outlier, however, was 5a, which displayed lower catalytic conversions than expected at 50 °C, given the binding strength of the ethereal "tail" and the steric bulk about the metal center. As discussed above, it is hypothesized that the multimetallic bridging species formed in solution are responsible for these observations. Furthermore, 5b showed slightly lower polymer chain lengths than expected, which became even shorter as the temperature was increased to 110 °C. This could be due to partial decomposition of pre-catalyst due to the more labile tail, which would lead to a slight excess of alcohol in solution. The excess alcohol could then act as a chain transfer agent to generate shorter polymer chains (as seen previously with 6a when 10 equiv of iPrOH was used). When the temperature of the reactions was increased to 110 °C, this also caused an increase in the PDIs seen for catalysts 5-8. This was best exemplified by 5b which displayed a PDI of 1.11 at 50 °C in comparison to 1.75 at 110 °C. We attribute this increase in PDI to a slower rate of reaction between the aluminum alkyl complexes and iPrOH versus a faster rate of insertion of caprolactone into an aluminum-alkoxide bond (polymer growth) at 110 °C. Notably, the increase in PDIs correlated more with thermal changes than any other factor: they did not correlate strongly with steric hindrance or the

donating ability of the scorpionate "tail". For example, at 50 °C, the PDIs were between 1.11 and 1.35, whereas, at 110 °C, they were generally between 1.72 and 1.84. The largest outlier was 5a with a PDI of 1.31 at 110 °C. It is proposed that 5a more uniformly activated at 110 °C than the other aluminum alkyl complexes, but the reason for this cleaner activation is still unknown. It could be linked to the weak binding ability of the ethereal hemilabile donor in 5a, along with the smaller steric size of the scorpionate ligand, but the bridging complexes seen in solution cannot be ruled out as a factor.

On the basis of the ROP results that were obtained, we propose a catalytic mechanism involving initial formation of an aluminum-alkoxide complex (supported by the incorporation of isopropoxy end groups into the PCL polymers, Figure S21), followed by de-coordination of the scorpionate "tail" prior to ε -CL coordination. As such, the aluminum center would alternate between 3- and 4-coordinate intermediates, as shown in Figure 6. It should be noted, however, that an alternative 5-coordinate pathway cannot be ruled out at this time, and further mechanistic studies are needed to differentiate between possible mechanisms.

CONCLUSION

In summary, a family of scorpionate ligands 1-4 were synthesized using a modular Friedel-Crafts alkylation reaction starting with commercially available reagents. The steric and electronic properties of the targeted compounds could be readily varied, and a wide range of "tail" groups could be incorporated, including imidazolyl, amino, and ethereal functionalities. This allowed the binding strength of the hemilabile neutral donor to be easily tuned. In order to investigate the binding modes of these ligands, they were combined with triethylaluminum to generate tetrahedral complexes 5-8. The variable binding strength of the scorpionate "tail" followed expected trends, with 5a forming bridging dimers in the solid state due to the weak donating ability of the ethereal moiety, and the decreased steric bulk ortho to the phenolate donors. Interestingly, the tridentate ligands displayed fairly flexible binding modes, with bond angles between 98° and 112°, indicating that they should be compatible with octahedral or trigonal bipyramidal coordination geometries. In addition, the aluminum alkyl complexes were found to be active catalysts for the ROP of ε -CL, both with and without the use of an alcohol co-catalyst. Higher activities and cleaner activations were seen, however, when 1 equiv of iPrOH was employed. Unsurprisingly, the steric size of the scorpionate ligand as well as the donating ability of the "tail" influenced the polymerization of ε -CL. Less sterically hindered complexes were able to polymerize ε -CL with more ease, as were species with more weakly bound neutral donors. It is believed that de-coordination of the scorpionate "tail" is required for polymerization and that the aluminum center alternates between 3- and 4-coordinate intermediates during the catalytic cycle, but more studies are needed to elucidate the mechanism of ROP with these systems.

■ EXPERIMENTAL SECTION

General Considerations. All procedures and manipulations were performed under an argon or nitrogen atmosphere using standard Schlenk-line and glovebox techniques unless stated otherwise. Solvents were dried and deoxygenated under argon using a LC Technology Solutions Inc. SP-1 stand-alone solvent purification system. All alcohols were dried and distilled over activated magnesium

(magnesium turnings and a crystal of iodine) under a nitrogen atmosphere. Deuterated solvents were purchased from Cambridge Isotope Laboratories, Sigma-Aldrich, Acros Organics, or Alfa Aesar degassed, and dried over activated molecular sieves prior to use. All other reagents were purchased from commercial sources and utilized without further purification unless stated otherwise. NMR spectra were recorded at ambient temperature and pressure using a Bruker 400 MHz spectrometer (400 MHz for ¹H, and 100 MHz for ¹³C). The ^1H and ^{13}C NMR spectra were measured relative to partially deuterated solvent peaks but are reported relative to tetramethylsilane (TMS). The variable temperature NMR spectra were recorded using a Bruker WB 600 MHz NMR-MRI spectrometer (600 MHz for ¹H). Spectra were processed and visualized with MestReNova v12.0.0-20080. The elemental analyses were performed at the University of Rochester, Department of Chemistry, on a PerkinElmer 2400 Series II Analyzer. Single-crystal X-ray data for compounds 2a and 7b were collected using a Bruker Proteum diffractometer equipped with dual CCD detectors (Apex II and Platinum 135) and a shared Bruker MicroStar microfocus rotating anode generator running at 45 mA and 60 kV (Cu K α λ = 1.54178 Å for **2a** and **7b**). The data collection strategy was calculated using the Bruker APEX2 software package to ensure desired data redundancy and percent completeness. Unit cell determination, initial indexing, data collection, frame integration, Lorentz-polarization corrections, and final cell parameter calculations were carried out using the Bruker APEX2 software package. An absorption correction was performed using SADABS. Single-crystal Xray data for compounds 5a, 6a,b, 7a, and 8a were collected using a Rigaku XtaLAB Synergy-S diffractometer equipped with a HyPix-6000HE Hybrid Photon Counting (HPC) detector and dual Mo and Cu microfocus sealed X-ray source (Mo K α λ = 0.71073 Å for 5a; Cu $K\alpha \lambda = 1.54184 \text{ Å for } 6a,b, 7a, \text{ and } 8a$). The data collection strategy was calculated using CrysAlisPro to ensure desired data redundancy and percent completeness. Unit cell determination, initial indexing, data collection, frame integration, Lorentz-polarization corrections, and final cell parameter calculations were carried out using CrysAlisPro. An absorption correction was performed using the SCALE3 ABSPACK scaling algorithm embedded within CrysAlisPro. The structures (2a, 5a, 6a,b, 7a,b, and 8a) were solved using the ShelXT structure solution program using Intrinsic Phasing and refined by Least Squares using the ShelXL program. All non-hydrogen atoms were refined anisotropically. Hydrogen atom positions were calculated geometrically and refined using the riding model. Olex2 was used for the preparation of the publication materials. The polymers were characterized by size exclusion chromatography (SEC) using an EcoSEC GPC system with an RI detector from TOSOH. The column set installed in this instrument consisted of the following three columns: 2 Tosoh TSKgel SuperMultiporeHZ-M; 4.6 × 150 mm; 4 μ m; and a TSKgel SuperMultiporeHZ-M guard. The calibration range was ≈600-1 000 000 Da using polystyrene standards. The operating flow rates were 0.35 mL/min for both the reference cell and the sample cell. Column temperature and detector temperature were set at 40 °C. Sample injection volume was 10 uL.

Synthesis of 1a ($C_{19}H_{24}O_3$). A mixture of 0.537 g (1 equiv, 3.62 mmol) of methoxyacetaldehyde diethylacetal and 0.885 g (2 equiv, 7.24 mmol) of 2,4-dimethylphenol in 10 mL of acetic acid was stirred for 15 min. The solution was then cooled to 0 $^{\circ}$ C, and 6.6 mL of 1:3 sulfuric acid:acetic acid was added. The reaction was allowed to stir for 2 days at room temperature. The reaction was then cooled to 0 °C and diluted with 20 mL of H_2O . The reaction was neutralized with 30 mL of 10 M NaOH, allowed to warm to room temperature, and then extracted three times using 50 mL of ethyl acetate. The organic layers were combined, then washed twice with 50 mL of water, dried with Na2SO4, filtered, and concentrated in vacuo. The product was stirred in 30 mL of hexanes, isolated by filtration, and washed with an additional 20 mL of hexanes to give a white solid. Yield: 0.569 g (52.4%). ¹H NMR (400 MHz, C_6D_6) δ : 6.87 (s, 2H, Aromatic-CH), 6.73 (s, 2H, Aromatic-CH), 6.14 (s, 2H, -OH), 4.78 (t, 1H, CHCH₂, J = 6.2 Hz), 3.80 (d, 2H, CHC H_2 , J = 6.2 Hz), 2.85 (s, 3H, O-C H_3), 2.12 (s, 6H, Aromatic- CH_3), and 2.08 (s, 6H, Aromatic- CH_3) ppm. ¹³C NMR (100 MHz, C_6D_6) δ : 151.02 (Aromatic-C), 130.70

(Aromatic-CH), 129.49 (Aromatic-C), 126.70 (Aromatic-CH), 125.60 (Aromatic-C), 77.54 (CHCH₂), 58.67 (O-CH₃), 40.34 (CHCH₂), 20.82 (Aromatic-CH₃), and 16.36 (Aromatic-CH₃) ppm. Anal. Calcd for $C_{19}H_{24}O_{3}$: C, 75.97; H, 8.05; N, 0.00. Found: C, 75.66; H, 8.27; N, 0.03.

Synthesis of 1b ($C_{25}H_{36}O_3$). A mixture of 0.541 g (1 equiv, 3.65 mmol) of methoxyacetaldehyde diethylacetal and 1.202 g (2 equiv, 7.32 mmol) of 2-tert-butyl-4-methylphenol in 10 mL of acetic acid was stirred for 15 min. The solution was then cooled to 0 °C, and 6.6 mL of 1:3 sulfuric acid:acetic acid was added. The reaction was allowed to stir for 2 days at room temperature. The reaction was then cooled to 0 $^{\circ}$ C and diluted with 20 mL of H_2 O. The reaction was neutralized with 30 mL of 10 M NaOH, allowed to warm to room temperature, and then extracted three times using 50 mL of ethyl acetate. The organic layers were combined, then washed twice with 50 mL of water, dried with Na₂SO₄, filtered, and concentrated in vacuo. The residue was recrystallized from cold hexanes to give a white solid. Yield: 0.355 g (25.2%). 1 H NMR (400 MHz, $C_{6}D_{6}$) δ: 7.12 (s, 2H, Aromatic-CH), 6.76 (s, 2H, Aromatic-CH), 6.30 (s, 2H, -OH), 4.55 (t, 1H, CHCH₂, J = 6.5 Hz), 3.65 (d, 2H, CHCH₂, J = 6.5 Hz), 2.75 (s, 3H, O-CH₃), 2.13 (s, 6H, Aromatic-CH₃), and 1.51 (s, 18H, C- $(CH_3)_3$) ppm. ¹³C NMR (100 MHz, C_6D_6) δ : 151.63 (Aromatic-C), 138.03 (Aromatic-C), 129.15 (Aromatic-C), 128.39 (Aromatic-C), 126.99 (Aromatic-CH), 125.77 (Aromatic-CH), 78.27 (CHCH₂), 58.40 (O-CH₃), 39.61 (CHCH₂), 34.70 (C-(CH₃)₃), 29.72 (C-(CH₃)₃), and 20.82 (Aromatic-CH₃) ppm. Anal. Calcd for C₂₅H₃₆O₃: C, 78.08; H, 9.44; N, 0.00. Found: C, 78.30; H, 9.61; N, 0.02.

Synthesis 2a·HCl (C₂₀H₂₇NO₂·HCl). A mixture of 0.594 g (1 equiv, 3.68 mmol) of dimethylaminoacetaldehyde diethylacetal and 0.884 g (2 equiv, 7.24 mmol) of 2,4-dimethylphenol in 10 mL of acetic acid was stirred for 15 min. The reaction was then cooled to 0 °C, and 6.6 mL of 1:3 sulfuric acid:acetic acid was added. The reaction was allowed to stir for 2 days at room temperature. The reaction was then cooled to 0 °C and was diluted with 20 mL of H₂O. The reaction was neutralized with 30 mL of 10 M NaOH, allowed to warm to room temperature, and then extracted three times using 50 mL of ethyl acetate. The organic layers were combined, then washed twice with 50 mL of water, dried with Na₂SO₄, filtered, and concentrated in vacuo. The residue was then dissolved in 50 mL of methanol, and 0.5 mL of 12 M HCl was added. After stirring for 15 min, the solvent was removed in vacuo. The residue was then stirred in 75 mL of ether for several hours, isolated by filtration, and washed with 20 mL of ether to give a white powder. Yield: 0.582 g (45.9%). ¹H NMR (400 MHz, DMSO- d_6) δ : 9.30 (s, 1H, -NH), 8.48 (s, 2H, -OH), 6.88 (s, 2H, Aromatic-CH), 6.81 (s, 2H, Aromatic-CH), 5.18 (t, 1H, CHCH₂, J = 7.4 Hz), 3.70 (d, 2H, CHCH₂, J = 7.4 Hz), 2.75 (s, 6H, N-(CH₃)₂), 2.16 (s, 6H, Aromatic-CH₃), and 2.15 (s, 6H, Aromatic-CH₃) ppm. ¹³C NMR (100 MHz, DMSO- d_6) δ : 150.50 (Aromatic-C), 130.41 (Aromatic-CH), 128.61 (Aromatic-C), 127.96 (Aromatic-C), 126.80 (Aromatic-CH), 125.66 (Aromatic-C), 59.79 (CHCH₂), 43.48 (N-(CH₃)₂), 34.03 (CHCH₂), 20.94 (Aromatic-CH₃), and 17.32 (Aromatic-CH₃) ppm. Anal. Calcd for [C₂₀H₂₈ClNO₂]0.25[H₂O]: C, 67.78; H, 8.11; N, 3.95. Found: C, 67.45; H, 8.21; N, 3.96.

Synthesis of 2b·HCl (C₂₆H₃₉NO₂·HCl). A mixture of 0.584 g (1 equiv, 3.62 mmol) of dimethylaminoacetaldehyde diethylacetal and 1.178 g (2 equiv, 7.17 mmol) of 2-tert-butyl-4-methylphenol in 10 mL of acetic acid was stirred for 15 min. The solution was then cooled to 0 $^{\circ}$ C, and 6.6 mL of 1:3 sulfuric acid:acetic acid was added. The reaction was allowed to stir for 2 days at room temperature. The reaction was then cooled to 0 °C and diluted with 20 mL of H₂O. The reaction was neutralized with 30 mL of 10 M NaOH, allowed to warm to room temperature, and then extracted three times using 50 mL of ethyl acetate. The organic layers were combined, then washed twice with 50 mL of water, dried with Na₂SO₄, filtered, and concentrated in vacuo. The residue was then dissolved in 50 mL of methanol, and 0.5 mL of 12 M HCl was added. After stirring for 15 min, the solvent was removed in vacuo. The residue was then dissolved using 75 mL of ether and stirred for several hours, causing the formation of a precipitate. The solid was isolated by filtration and washed with 20

mL of ether to give a white powder. Yield: 0.622 g (39.5%). $^{1}{\rm H}$ NMR (400 MHz, DMSO- d_6) δ : 9.08 (s, 1H, -NH), 8.75 (s, 2H, -OH), 6.95–6.90 (m, 4H, Aromatic-CH), 5.34 (t, 1H, CHCH₂, J = 7.5 Hz), 3.80 (app. t, 2H, CHCH₂), 2.80 (d, 6H, N-(CH₃)₂, J = 4.8 Hz), 2.21 (s, 6H, Aromatic-CH₃), and 1.34 (s, 18H, C-(CH₃)₃) ppm. $^{13}{\rm C}$ NMR (100 MHz, DMSO- d_6) δ : 150.42 (Aromatic-C), 139.39 (Aromatic-C), 129.63 (Aromatic-C), 126.52 (Aromatic-C), 125.71 (Aromatic-CH), 59.58 (CHCH₂), 44.16 (N-(CH₃)₂), 35.00 (C-(CH₃)₃), 33.56 (CHCH₂), 30.28 (C-(CH₃)₃), and 21.42 (Aromatic-CH₃) ppm. Anal. Calcd for C₂₆H₄₀ClNO₂:0.5(H₂O): C, 70.48; H, 9.33; N, 3.16. Found: C, 70.68; H, 9.47; N, 3.20.

Synthesis of 2a (C₂₀H₂₇NO₂). A suspension of 0.0355 g of LiOH (1 equiv, 1.48 mmol) in 5 mL of DCM was added to 0.513 g of MAEMP·HCl (1 equiv, 1.47 mmol) in 5 mL of DCM. The solution was stirred for 2 h and then filtered through Celite. The filtrate was dried using Na₂SO₄ and filtered, and the solvent was removed in vacuo. The product was isolated as a white solid. Yield: 0.295 g (64.1%). Crystals suitable for X-ray diffraction studies were grown from the slow diffusion of pentane into a toluene solution of 2a at -30 °C. ¹H NMR (400 MHz, D₂O) δ : 6.96 (s, 2H, Aromatic-CH), 6.94 (s, 2H, Aromatic-CH), 5.18 (t, 1H, CHCH₂, J = 8.0 Hz), 3.78 (d, 2H, CHC H_2 , J = 8.0 Hz), 2.91 (s, 6H, N-(C H_3)₂), 2.19 (s, 6H, Aromatic-CH₃), 2.18 (s, 6H, Aromatic-CH₃) ppm. ¹³C NMR (100 MHz, D₂O) δ : 148.77 (Aromatic-C), 131.28 (Aromatic-C), 130.68 (Aromatic-CH), 126.87 (Aromatic-C), 126.60 (Aromatic-C), 125.86 (Aromatic-CH), 60.44 (CHCH₂), 43.31 (N-(CH₃)₂), 33.41 (CHCH₂), 19.51 (Aromatic-CH₃), 15.63 (Aromatic-CH₃) ppm. Anal. Calcd for C₂₀H₂₇NO₂: C, 76.64; H, 8.68; N, 4.47. Found: C, 76.70; H, 8.95; N, 4.42.

Synthesis of 2b ($C_{26}H_{39}NO_2$). A suspension of 0.0316 g of LiOH (1 equiv, 1.32 mmol) in 5 mL of DCM was added to 0.567 g of MAETBMP·HCl (1 equiv, 1.31 mmol) in 5 mL of DCM. The solution was stirred for 2 h and then filtered through Celite. The filtrate was dried using Na₂SO₄ and filtered, and the solvent was removed in vacuo. The product was isolated as a white solid. Yield: 0.375 g (72.1%). ¹H NMR (400 MHz, DMSO- d_6) δ : 9.20 (br s, 2H, -OH), 6.84 (s, 2H, Aromatic-CH), 6.46 (s, 2H, Aromatic-CH), 4.76 (t, 1H, CHCH₂, J = 5.7 Hz), 2.96 (d, 2H, CHCH₂, J = 5.6 Hz), 2.33 (s, 6H, N-(CH₃)₂), 2.10 (s, 6H, Aromatic-CH₃), and 1.36 (s, 18H, C- $(CH_3)_3$) ppm. ¹³C NMR (100 MHz, DMSO- d_6) δ : 152.47 (Aromatic-C), 137.94 (Aromatic-C), 132.34 (Aromatic-C), 127.31 (Aromatic-CH), 127.01 (Aromatic-C), 125.55 (Aromatic-CH), 67.03 (CHCH₂), 45.32 (N-(CH₃)₂), 38.46 (CHCH₂), 34.96 (C-(CH₃)₃), 30.29 (C-(CH₃)₃), and 21.39 (Aromatic-CH₃) ppm. Anal. Calcd for C₂₆H₃₉NO₂: C, 78.54; H, 9.89; N, 3.52. Found: C, 78.19; H, 10.05; N, 3.57.

Synthesis of 3a ($C_{20}H_{22}N_2O_2$). A mixture of 0.325 g (1 equiv, 3.39 mmol) of 2-imidazolecarboxaldehyde and 0.877 g (2 equiv, 7.18 mmol) of 2,4-dimethylphenol in 10 mL of acetic acid was stirred for 15 min. The solution was then cooled to 0 °C, and 6.6 mL of 1:3 sulfuric acid:acetic acid was added. The reaction was allowed to stir for 2 days at room temperature. The reaction was then cooled to 0 $^{\circ}$ C and diluted with 20 mL of H₂O. The reaction was neutralized with 30 mL of 10 M NaOH, allowed to warm to room temperature, and then extracted three times using 50 mL of ethyl acetate. The organic layers were combined, then washed twice with 50 mL of water, dried with Na₂SO₄, filtered, and concentrated in vacuo. The resulting residue was washed through a silica gel plug using 5% ethyl acetate in hexanes. The silica gel plug was then washed with ethyl acetate to elute the product. The resulting filtrate was concentrated in vacuo to give a white solid. Yield: 0.519 g (47.5%). ¹H NMR (400 MHz, DMSO-*d*₆) δ: 10.76 (br s, 3H, -OH, -NH), 7.00 (s, 2H, Imidazole-CH), 6.88 (s, 2H, Aromatic-CH), 6.75 (s, 2H, Aromatic-CH), 5.75 (s, 1H, CH), and 2.11 (s, 12H, Aromatic-CH₃) ppm. ¹³C NMR (100 MHz, DMSO-d₆) δ: 150.72 (Aromatic-C), 149.64 (Aromatic-C), 129.74 (Aromatic-CH), 128.24 (Aromatic-CH), 127.52 (Aromatic-C), 126.81 (Aromatic-C), 125.16 (Aromatic-C), 120.87 (Imidazole-CH), 42.34 (CH), 21.13 (Aromatic-CH₃), and 16.77 (Aromatic-CH₃) ppm. Anal. Calcd for $C_{20}H_{22}N_2O_2 \cdot 0.25(H_2O)$: C, 73.48; H, 6.94; N, 8.57. Found: C, 73.31; H, 7.00; N, 8.71.

Synthesis of 3b ($C_{26}H_{34}N_2O_2$). A mixture of 0.329 g (1 equiv, 3.42 mmol) of 2-imidazolecarboxaldehyde and 1.104 g (2 equiv, 6.72 mmol) of 2-tert-butyl-4-methylphenol in 10 mL of acetic acid was stirred for 15 min. The solution was then cooled to 0 $^{\circ}$ C, and 6.6 mL of 1:3 sulfuric acid:acetic acid was added. The reaction was allowed to stir for 2 days at room temperature. The reaction was then cooled to 0 °C and diluted with 20 mL of H₂O. The reaction was neutralized with 30 mL of 10 M NaOH, allowed to warm to room temperature, and then extracted three times using 50 mL of ethyl acetate. The organic layers were combined, then washed twice with 50 mL of water, dried with Na2SO4, filtered, and concentrated in vacuo. The resulting residue was washed through a silica gel plug using 5% ethyl acetate in hexanes. The silica gel plug was then washed with ethyl acetate to elute the product. The resulting filtrate was concentrated in vacuo to give a residue, which was dissolved in pentane, filtered, and then dried under reduced pressure to give a white solid. Yield: 0.337 g (24%). ¹H **NMR** (400 MHz, DMSO- d_6) δ : 10.75 (s, 2H, -OH), 7.01 (s, 4H, Aromatic-CH), 6.88 (s, 2H, Imidazole-CH), 5.79 (s, 1H, CH), 2.12 (s, 6H, Aromatic-CH₃), and 1.35 (s, 18H, C-(CH₃)₃) ppm. ¹³C NMR (100 MHz, DMSO-d₆) δ: 151.59 (Aromatic-C), 149.88 (Aromatic-C), 138.81 (Aromatic-C), 129.83 (Aromatic-C), 129.03 (Aromatic-CH), 127.90 (Aromatic-C), 126.42 (Imidazole-CH), 121.34 (Aromatic-CH), 43.47 (CH), 35.02 (C-(CH₃)₃), 30.34 (C-(CH₃)₃), and 21.22 (Aromatic-CH $_3$) ppm. Anal. Calcd for $C_{26}H_{34}N_2O_2$: C, 76.81; H, 8.43; N, 6.89. Found: C, 76.59; H, 8.63; N, 6.76.

Synthesis of 4a ($C_{21}H_{24}N_2O_2$). A mixture of 0.385 g (1 equiv, 3.50 mmol) of 1-methyl-2-imidazolecarboxaldehyde and 0.851 g (2 equiv, 6.96 mmol) of 2,4-dimethylphenol in 10 mL of acetic acid was stirred for 15 min. The solution was then cooled to 0 °C, and 6.6 mL of 1:3 sulfuric acid:acetic acid was added. The reaction was allowed to stir for 2 days at room temperature. The reaction was then cooled to 0 $^{\circ}$ C and diluted with 20 mL of H_2O . The reaction was neutralized with 30 mL of 10 M NaOH, allowed to warm to room temperature, and then extracted three times using 50 mL of ethyl acetate. The organic layers were combined, then washed twice with 50 mL of water, dried with Na2SO4, filtered, and concentrated in vacuo. The resulting oil was dissolved in 20 mL of 5% ethyl acetate in hexanes and stirred, causing the formation of a precipitate. The resulting suspension was filtered and washed with minimal hexanes to yield the product as a white solid. Yield: 0.438 g (37.4%). 1 H NMR (400 MHz, DMSO- d_{6}) δ: 10.00 (s, 2H, -OH), 7.11 (s, 1H, Imidazole-CH), 6.87 (s, 1H, Imidazole-CH), 6.84 (s, 2H, Aromatic-CH), 6.76 (s, 2H, Aromatic-CH), 5.79 (s, 1H, CH), 3.63 (s, 3H, N-CH₃), 2.11 (s, 6H, Aromatic-CH₃), and 2.10 (s, 6H, Aromatic-CH₃) ppm. ¹³C NMR (100 MHz, DMSO- d_6) δ : 151.18 (Aromatic-C), 150.09 (Aromatic-C), 130.34 (Aromatic-CH), 128.x71 (Aromatic-CH), 127.47 (Aromatic-C), 125.67 (Aromatic-C), 125.00 (Imidazole-CH), 121.70 (Imidazole-CH), 33.01 (N-CH₃), 20.82 (Aromatic-CH₃), and 17.21 (Aromatic-CH₃) ppm. Anal. Calcd for C₂₁H₂₄N₂O₂·0.25(H₂O): C, 73.98; H, 7.24; N, 8.22. Found: C, 74.23; H, 7.19; N, 8.19.

Synthesis of 4b ($C_{27}H_{36}N_2O_2$). A mixture of 0.395 g (1 equiv, 3.6 mmol) of 1-methyl-2-imidazolecarboxaldehyde and 1.193 g (2 equiv, 7.3 mmol) of 2-tert-butyl-4-methylphenol in 10 mL of acetic acid was stirred for 15 min. The solution was then cooled to 0 $^{\circ}\text{C}\textsc{,}$ and 6.6 mL of 1:3 sulfuric acid:acetic acid was added. The reaction was allowed to stir for 2 days at room temperature. The reaction was then cooled to 0 °C and diluted with 20 mL of H₂O. The reaction was neutralized with 30 mL of 10 M NaOH, allowed to warm to room temperature, and then extracted three times using 50 mL of ethyl acetate. The organic layers were combined, then washed twice with 50 mL of water, dried with Na₂SO₄, filtered, and concentrated in vacuo. The resulting oil was dissolved in 20 mL of 5% ethyl acetate in hexanes and stirred. The resulting solution was filtered to yield the solid product as a white powder. Yield: 0.627 g (49%). Crystals suitable for X-ray diffraction studies were grown from a toluene solution of 4b cooled to -30 °C. ¹H NMR (400 MHz, C_6D_6) δ : 10.07 (s, 2H, -OH), 7.10 (s, 2H, Aromatic-CH), 6.91 (s, 2H, Aromatic-CH), 6.72 (s, 1H, Imidazole-CH), 5.94 (s, 1H, Imidazole-CH), 5.11 (s, 1H, CH), 2.54 (s, 3H, N- CH_3), 2.15 (s, 6H, Aromatic- CH_3), and 1.50 (s, 18 H, C- $(CH_3)_3$) ppm. ¹³C NMR (100 MHz, C_6D_6) δ : 152.32 (Aromatic-C), 149.00 (Aromatic-C), 139.84 (Aromatic-C), 128.74 (Aromatic-CH), 128.64 (Aromatic-CH), 124.92(Imidazole-CH), 120.59 (Imidazole-CH), 47.32 (CH), 34.86 (C-(CH₃)₃), 31.84 (N-CH₃), 29.80 (C-(CH₃)₃), and 20.72 (Aromatic-CH₃) ppm. Anal. Calcd for C₂₇H₃₆N₂O₂: C, 77.104; H, 8.63; N, 6.66. Found: C, 76.78; H, 8.74; N, 6.65.

Synthesis of 5a (Al(Et)(1a)). To a solution of 90.3 mg of 1a (1 equiv, 0.300 mmol) in 6 mL of benzene was added 0.30 mL of 1.0 M Al(Et)₃ in hexanes (1 equiv, 0.30 mmol), and the mixture was stirred for 10 min. The solvent was then removed in vacuo, and the resulting residue was stirred in 5 mL of pentane for an hour. The product was then isolated as a white solid by filtration and washed with minimal pentane to give a white powder. Yield: 55.2 mg (52.0%). Crystals suitable for X-ray diffraction studies were grown from the slow evaporation of a benzene solution of 5a at room temperature. Note that the following spectroscopic characterization is only for the major monometallic species that was identified in the solution. Other minor species were also present but could not be fully characterized due to their low concentrations. ¹H NMR (400 MHz, C_6D_6) δ : 6.87 (s, 2H, Aromatic-CH), 6.77 (s, 2H, Aromatic-CH), 3.71-3.67 (m, 3H, CHCH₂, CHCH₂), 2.46 (s, 3H, O-CH₃), 2.38 (s, 6H, Aromatic-CH₃), 2.18 (s, 6H, Aromatic-CH₃), 1.43 (t, 3H, Al-CH₂CH₃, J = 8.2 Hz), and 0.30 (q, 2H, Al-CH₂CH₃, J = 8.2 Hz) ppm. ¹³C NMR (100 MHz, C_6D_6) δ : 154.67 (Aromatic-C), 131.26 (Aromatic-CH), 129.67 (Aromatic-CH), 129.05 (Aromatic-C), 128.59 (Aromatic-C), 126.98 (Aromatic-C), 83.61 (CHCH₂), 60.80 (O-CH₃), 51.71 (CHCH₂), 20.64 (Aromatic-CH₃), 17.38 (Aromatic-CH₃), 8.81 (Al-CH₂CH₃), and -4.96 (Al-CH₂CH₃) ppm. Anal. Calcd for AlC₂₁H₂₇O₃: C, 71.17; H, 7.68; N, 0.00. Found: C, 70.81; H, 7.94; N, -0.19.

Synthesis of 5b (Al(Et)(1b)). To a solution of 113.2 mg of 1b (1 equiv, 0.30 mmol) in 6 mL of benzene was added 0.30 mL of 1.0 M Al(Et)₃ in hexanes (1 equiv, 0.30 mmol), and the mixture was stirred overnight. The solvent was then removed in vacuo, and the resulting residue was stirred in 5 mL of pentane for an hour. The product was then isolated as a white solid by filtration and washed with minimal pentane. Yield: 107 mg (82.3%). ¹H NMR (400 MHz, C_6D_6) δ : 7.13 (s, 2H, Aromatic-CH), 6.78 (s, 2H, Aromatic-CH), 3.72-3.69 (m, 3H, CHCH₂, CHCH₂), 2.51 (s, 3H, O-CH₃), 2.19 (s, 6H, Aromatic- CH_3), 1.60 (s, 18H, $C-(CH_3)_3$), 1.51 (t, 3H, $Al-CH_2CH_3$, J = 8.2 Hz), and 0.35 (q, 2H, Al-C H_2 C H_3 , J = 8.2 Hz) ppm. ¹³C NMR (100 MHz, C_6D_6) δ : 155.23 (Aromatic-C), 139.65 (Aromatic-C), 130.18 (Aromatic-C), 130.01 (Aromatic-CH), 127.45 (Aromatic-C), 126.79 (Aromatic-CH), 83.41 (CHCH₂), 60.77 (O-CH₃), 52.27 (CHCH₂), 35.33 (C-(CH₃)₃), 30.15 (C-(CH₃)₃), 20.99 (Aromatic-CH₃), 8.73 (Al-CH₂CH₃), and -4.69 (Al-CH₂CH₃) ppm. Anal. Calcd for AlC₂₇H₃₉O₃: C, 73.94; H, 8.96; N, 0.00. Found: C, 73.70; H, 9.12; $N_{\cdot \cdot} - 0.17$.

Synthesis of 6a (Al(Et)(2a)). To a solution of 95.0 mg of 2a (1 equiv, 0.30 mmol) in 6 mL of benzene was added 0.30 mL of 1.0 M Al(Et)₃ in hexanes (1 equiv, 0.30 mmol), and the mixture was stirred overnight. The solvent was then removed in vacuo, and the resulting residue was stirred in 5 mL of pentane for an hour. The product was then isolated as a white solid by filtration and washed with minimal pentane. Yield: 92.9 mg (83.3%). Crystals suitable for X-ray diffraction studies were grown from a toluene solution of 6a cooled to -30 °C. ¹H NMR (400 MHz, C_6D_6) δ : 6.84 (s, 2H, Aromatic-CH), 6.78 (s, 2H, Aromatic-CH), 3.71 (t, 1H, CHCH₂, J = 3.9 Hz), 2.66 (d, 2H, CHC H_2 , J = 3.9 Hz), 2.37 (s, 6H, Aromatic-C H_3) 2.17 (s, 6H, Aromatic-CH₃), 1.68 (s, 6H, N-(CH₃)₂), 1.49 (t, 3H, Al- CH_2CH_3 , J = 8.2 Hz), and 0.28 (q, 2H, Al- CH_2CH_3 , J = 8.2 Hz) ppm. ¹³C NMR (100 MHz, C_6D_6) δ : 154.80 (Aromatic-C), 130.98 (Aromatic-CH), 129.62 (Aromatic-C) 129.52 (Aromatic-CH), 128.78 (Aromatic-C), 126.90 (Aromatic-C), 66.40 (CHCH₂), 50.55 (CHCH₂), 46.35 (N-(CH₃)₂), 20.68 (Aromatic-CH₃), 17.32 (Aromatic-CH₃), 9.44 (Al-CH₂CH₃), and -4.63 (Al-CH₂CH₃) ppm. Anal. Calcd for AlC₂₂H₃₀NO₂: C, 71.91; H, 8.23; N, 3.81. Found: C, 71.89; H, 8.20; N, 3.90.

Synthesis of 6b (Al(Et)(2b)). To a solution of 236 mg of 2b (1 equiv, 0.595 mmol) in 12 mL of benzene was added 0.60 mL of 1.0 M $Al(Et)_3$ in hexanes (1 equiv, 0.60 mmol), and the mixture was stirred overnight. The solvent was then removed in vacuo, and the product

was dissolved in 1 mL of pentane. Upon cooling to -30 °C, a precipitate formed, which was isolated by filtration and washed with 1 mL of cold pentane to give a white powder. Yield: 72.5 mg (27.1%). Crystals suitable for X-ray diffraction studies were grown from a pentane solution of 6b cooled to -30 °C. ¹H NMR (400 MHz, C_6D_6) δ : 7.11 (s, 2H, Aromatic-CH), 6.80 (s, 2H, Aromatic-CH), 3.72 (t, 1H, CHCH₂, J = 3.9 Hz), 2.60 (d, 2H, CHCH₂, J = 3.9 Hz), 2.19 (s, 6H, Aromatic-CH₃), 1.68 (s, 6H, N-(CH₃)₂), 1.59 (s, 18H, $C(CH_3)_3$) 1.54 (t, 3H, Al-CH₂CH₃, J = 8.2 Hz), and 0.29 (q, 2H, Al- CH_2CH_3 , J = 8.2 Hz) ppm. ¹³C NMR (100 MHz, C_6D_6) δ : 155.33 (Aromatic-C), 139.32 (Aromatic-C), 131.19 (Aromatic-C), 130.11 (Aromatic-CH), 127.13 (Aromatic-C), 126.67 (Aromatic-CH), 66.20 (CHCH₂), 51.16 (CHCH₂), 46.20 (N-(CH₃)₂), 35.30 (C-(CH₃)₃), 30.03 (C-(CH₃)₃), 21.02 (Aromatic-CH₃), 9.27 (Al-CH₂CH₃), and -4.52 (Al-CH₂CH₃) ppm. Anal. Calcd for AlC₂₈H₄₂NO₂: C, 74.47; H, 9.37; N, 3.10. Found: C, 74.35; H, 9.70; N, 2.92.

Synthesis of 7a (Al(Et)(3a)). To a solution of 96.8 mg of 3a (1 equiv, 0.30 mmol) in 6 mL of benzene was added 0.30 mL of 1.0 M Al(Et)₃ in hexanes (1 equiv, 0.30 mmol), and the mixture was stirred overnight. The solvent was then removed in vacuo, and the resulting residue was stirred in 5 mL of pentane for an hour. The product was then isolated as a white solid by filtration and washed with minimal pentane. Yield: 59.3 mg (52.5%). Crystals suitable for X-ray diffraction studies were grown from a toluene solution of 7a cooled to -30 °C. ¹H NMR (400 MHz, C₆D₆) δ : 7.99 (s, 1H, -NH), 6.83 (s, 2H, Aromatic-CH), 6.81 (s, 2H, Aromatic-CH), 6.20 (s, 1H, Imidazole-CH), 5.65 (s, 1H, Imidazole-CH), 4.45 (s, 1H, CH), 2.32 (s, 6H, Aromatic-CH₃), 2.21 (s, 6H, Aromatic-CH₃), 1.64 (t, 3H, Al-CH₂CH₃, J = 8.2 Hz), and 0.77 (q, 2H, Al-CH₂CH₃, J = 8.2 Hz) ppm. ¹³C NMR (100 MHz, C_6D_6) δ : 154.69 (Aromatic-C), 149.17 (Aromatic-C), 131.48 (Aromatic-CH), 130.22 (Aromatic-C), 129.22 (Aromatic-CH), 126.14 (Aromatic-C), 125.64 (Aromatic-C), 122.86 (Imidazole-CH), 115.39 (Imidazole-CH), 51.77 (CH), 20.24 (Aromatic-CH₃), 17.15 (Aromatic-CH₃), 8.98 (Al-CH₂CH₃), and -4.65 (Al-CH₂CH₃) ppm. Anal. Calcd for AlC₂₂H₂₅N₂O₂: C, 70.20; H, 6.69; N, 7.44. Found: C, 70.54; H, 6.92; N, 7.47.

Synthesis of 7b (Al(Et)(3b)). To a solution of 119 mg of 3b (1 equiv, 0.29 mmol) in 6 mL of benzene was added 0.30 mL of 1.0 M Al(Et)₃ in hexanes (1 equiv, 0.30 mmol), and the mixture was stirred overnight. The solvent was then removed in vacuo, and the resulting residue was stirred in 5 mL of pentane for an hour. The product was then isolated as a white solid by filtration and washed with minimal pentane. Yield: 80.2 mg (59.2%). Crystals suitable for X-ray diffraction studies were grown from the slow diffusion of pentane into a toluene solution of 7b at -30 °C. ¹H NMR (400 MHz, C_6D_6) δ: 7.81 (s, 1H, -NH), 7.15 (s, 2H, Aromatic-CH), 6.89 (s, 2H, Aromatic-CH), 6.21 (s, 1H, Imidazole-CH), 5.67 (s, 1H, Imidazole-CH), 4.56 (s, 1H, CH), 2.25 (s, 6H, Aromatic-CH₃) 1.71 (t, 3H, Al- CH_2CH_3 , J = 8.2 Hz), 1.57 (s, 18H, C-(CH_3)₃), and 0.72 (q, 2H, Al- CH_2CH_3 , J = 8.2 Hz) ppm. ¹³C NMR (100 MHz, C_6D_6) δ : 155.81 (Aromatic-C), 149.65 (Aromatic-C), 141.13 (Aromatic-C), 130.11 (Aromatic-CH), 128.59 (Aromatic-C), 127.63 (Aromatic-CH), 126.45 (Aromatic-C), 123.17 (Imidazole-CH), 115.78 (Imidazole-CH), 52.56 (CH), 35.53 (C-(CH₃)₃), 30.06 (C-(CH₃)₃), 20.96(Aromatic-CH₃), 9.40 (Al-CH₂CH₃), and -4.22 (Al-CH₂CH₃) ppm. Anal. Calcd for AlC₂₈H₃₇N₂O₂: C, 73.02; H, 8.10; N, 6.08. Found: C, 72.88; H, 7.90; N, 5.99.

Synthesis of 8a (Al(Et)(4a)). To a solution of 102 mg of 4a (1 equiv, 0.30 mmol) in 6 mL of benzene was added 0.30 mL of 1.0 M Al(Et)₃ in hexanes (1 equiv, 0.30 mmol), and the mixture was stirred overnight. The solvent was then removed in vacuo, and the resulting residue was stirred in 5 mL of pentane for an hour. The product was then isolated as a white solid by filtration and washed with minimal pentane. Yield: 76.2 mg (65%). Crystals suitable for X-ray diffraction studies were grown from the slow diffusion of pentane into a toluene solution of 8a at -30 °C. ¹H NMR (400 MHz, C_6D_6) δ : 6.88 (s, 2H, Aromatic-CH), 6.85 (s, 2H, Aromatic-CH), 6.33 (s, 1H, Imidazole-CH), 4.79 (s, 1H, CH), 2.39 (s, 6H, Aromatic-CH₃), 2.24 (s, 3H, N-CH₃), 2.21 (s, 6H, Aromatic-CH₃), 1.71 (t, 3H, Al-CH, CH_3) I = 8.2 Hz), and 0.75 (q, 2H, Al-CH, CH_3), I = 8.2 Hz), and 0.75 (q, 2H, Al-CH, I = 8.2 Hz), and 0.75 (q, 2H, Al-CH, I = 8.2 Hz), and 0.75 (q, 2H, Al-CH, I = 8.2 Hz), and 0.75 (q, 2H, Al-CH, I = 8.2 Hz), and 0.75 (q, 2H, Al-CH, I = 8.2 Hz), and 0.75 (q, 2H, Al-CH, I = 8.2 Hz), and 0.75 (q, 2H, Al-CH, I = 8.2 Hz), and 0.75 (q, 2H, Al-CH, I = 8.2 Hz), and 0.75 (q, 2H, Al-CH, I = 8.2 Hz), and 0.75 (q, 2H, Al-CH, I = 8.2 Hz), and 0.75 (q, 2H, Al-CH, I = 8.2 Hz), and 0.75 (q, 2H, Al-CH, I = 8.2 Hz).

= 8.2 Hz) ppm. 13 C NMR (100 MHz, C_6D_6) δ : 155.67 (Aromatic-C), 149.40 (Aromatic-C), 131.93 (Aromatic-C), 130.74 (Aromatic-CH), 129.72 (Aromatic-CH), 126.10 (Aromatic-C), 125.29 (Aromatic-C), 121.58 (Imidazole-CH), 120.96 (Imidazole-CH), 49.95 (CH), 32.38 (N-CH₃), 20.64 (Aromatic-CH₃), 17.96 (Aromatic-CH₃), 9.50 (Al-CH₂CH₃), and -4.28 (Al-CH₂CH₃) ppm. Anal. Calcd for AlC₂₃H₂₉N₂O₂: C, 70.75; H, 6.97; N, 7.18. Found: C, 70.83; H, 6.86; N, 7.16.

Synthesis of 8b (Al(Et)(4b)). To a solution of 128 mg of 4b (1 equiv, 0.30 mmol) in 6 mL of benzene was added 0.30 mL of 1.0 M Al(Et)₃ in hexanes (1 equiv, 0.30 mmol), and the mixture was stirred overnight at 70 °C. The solvent was then removed in vacuo, and the resulting residue was stirred in 5 mL of pentane for an hour. The product was then isolated as a white solid by filtration and washed with minimal pentane. Yield: 84.1 mg (59%). ¹H NMR (400 MHz, C_6D_6) δ : 7.17 (s, 2H, Aromatic-CH), 6.89 (s, 2H, Aromatic-CH), 6.33 (s, 2H, Imidazole-CH), 5.31 (s, 1H, Imidazole-CH), 4.82 (s, 1H, CH), 2.25 (s, 6H, Aromatic-CH₃), 2.18 (s, 3H, N-CH₃), 1.79 (t, 3H, Al-CH₂CH₃, J = 8.2 Hz), 1.64 (s, 18H, C(CH₃)₃), and 0.80 (q, 2H, Al-CH₂CH₃, J = 8.2 Hz) ppm. ¹³C NMR (100 MHz, C₆D₆) δ : 156.44 (Aromatic-C), 149.36 (Aromatic-C), 141.06 (Aromatic-C), 130.21 (Aromatic-CH), 128.59 (Aromatic-C), 127.08 (Aromatic-C), 125.89 (Aromatic-C), 121.22 (Imidazole-CH), 121.09 (Imidazole-CH), 50.31 (CH), 35.58 (C-(CH₃)₃)), 32.34 (N-CH₃), 30.05 (C- $(CH_3)_3$, 21.00 (Aromatic-CH₃), 9.53 (Al-CH₂CH₃), and -4.36 (Al-CH₂CH₃) ppm. Anal. Calcd for AlC₂₉H₃₉N₂O₂: C, 73.39; H, 8.28; N, 5.90. Found: C, 73.40; H, 8.19; N, 5.52.

General Procedure for ROP of ε -CL. Stock solutions of aluminum catalyst (0.0133 M), iPrOH (0.08 M), and ε -CL (8 M) in toluene were prepared. 0.75 mL of the aluminum stock solution was added to a Schlenk flask and cycled onto a Schlenk line. The solution was heated for 5 min at the desired temperature. 0.125 mL of the iPrOH stock solution and 0.125 mL of the $\varepsilon\text{-CL}$ stock solution were then added. The reaction was allowed to stir at the desired temperature for 1 h and then quenched with 0.35 mL of a 3% acetic acid in ether solution. The solvent was removed in vacuo, and the solid was analyzed using ¹H NMR spectroscopy. The solid was then washed with hexanes and dried. The final concentrations in the catalytic mixture were 0.01 M catalyst, 0.01 M iPrOH, and 1 M ε -CL. For GPC-SEC analysis, polymer solutions were prepared in THF to make a final concentration of about 1-1.5 mg/mL. The samples were allowed to dissolve for 1-2 h and filtered through 0.2 µm pore size PTFE filters into autosampler vials. Some samples were sonicated for 30 s to facilitate dissolution prior to filtration. The spectra were analyzed using the EcoSEC Analysis software.

ASSOCIATED CONTENT

Supporting Information

The Supporting Information is available free of charge at https://pubs.acs.org/doi/10.1021/acs.organomet.1c00400.

 1 H NMR spectra for 1–8. Variable temperature 1 H NMR spectra for 5a. Representative 1 H NMR spectra for polycaprolactone samples generated with and without a co-catalyst. Complete set of data for the ROP of ε-caprolactone using 5–8. Crystallographic data tables for 2a, 4b, 5a, 6a–b, 7a–b, and 8a (PDF)

Accession Codes

CCDC 2094139–2094146 contain the supplementary crystallographic data for this paper. These data can be obtained free of charge via www.ccdc.cam.ac.uk/data_request/cif, or by emailing data_request@ccdc.cam.ac.uk, or by contacting The Cambridge Crystallographic Data Centre, 12 Union Road, Cambridge CB2 1EZ, UK; fax: +44 1223 336033.

AUTHOR INFORMATION

Corresponding Author

Peter E. Sues — Department of Chemistry, Kansas State University, Manhattan, Kansas 66503, United States; orcid.org/0000-0002-3975-119X; Email: psues@ksu.edu

Authors

Elizabeth N. Cooper — Department of Chemistry, Kansas State University, Manhattan, Kansas 66503, United States Boris Averkiev — Department of Chemistry, Kansas State University, Manhattan, Kansas 66503, United States Victor W. Day — Department of Chemistry, University of Kansas, Lawrence, Kansas 66045, United States

Complete contact information is available at: https://pubs.acs.org/10.1021/acs.organomet.1c00400

Notes

The authors declare no competing financial interest.

ACKNOWLEDGMENTS

We would like to acknowledge the NSF-MRI grants CHE-0923449 and CHE-2018414, which were used to purchase the single-crystal X-ray diffractometers and associated software employed in this study, as well as the NSF-MRI grants CHE-1826982 and CHE-1337438, which were used to purchase the Bruker 400 and 600 MHz spectrometers, respectively. We would also like to thank Dr. Katrina Pangilinan from the Polymer Characterization Laboratory at the University of Tennessee, Knoxville, for performing the GPC-SEC analysis, as well as Dr. William Brennessel from the CENTC Elemental Analysis Facility at the University of Rochester, for performing the elemental analyses.

REFERENCES

- (1) Xu, W.; Chen, W.-Q.; Jiang, D.; Zhang, C.; Ma, Z.; Ren, Y.; Shi, L. Evolution of the Global Polyethylene Waste Trade System. *Ecosyst. Health Sustain.* **2020**, *6* (1), 1756925.
- (2) Jubinville, D.; Esmizadeh, E.; Saikrishnan, S.; Tzoganakis, C.; Mekonnen, T. A Comprehensive Review of Global Production and Recycling Methods of Polyolefin (PO) Based Products and Their Post-Recycling Applications. Sustain. Mater. Techno. 2020, 25, e00188.
- (3) Lebreton, L.; Slat, B.; Ferrari, F.; Sainte-Rose, B.; Aitken, J.; Marthouse, R.; Hajbane, S.; Cunsolo, S.; Schwarz, A.; Levivier, A.; Noble, K.; Debeljak, P.; Maral, H.; Schoeneich-Argent, R.; Brambini, R.; Reisser, J. Evidence That the Great Pacific Garbage Patch Is Rapidly Accumulating Plastic. Sci. Rep. 2018, 8 (1), 4666.
- (4) Law, K. L.; Morét-Ferguson, S. E.; Goodwin, D. S.; Zettler, E. R.; DeForce, E.; Kukulka, T.; Proskurowski, G. Distribution of Surface Plastic Debris in the Eastern Pacific Ocean from an 11-Year Data Set. *Environ. Sci. Technol.* **2014**, *48* (9), 4732–4738.
- (5) Jambeck, J. R.; Geyer, R.; Wilcox, C.; Siegler, T. R.; Perryman, M.; Andrady, A.; Narayan, R.; Law, K. L. Plastic Waste Inputs from Land into the Ocean. *Science* **2015**, 347 (6223), 768–771.
- (6) Eriksen, M.; Lebreton, L. C. M.; Carson, H. S.; Thiel, M.; Moore, C. J.; Borerro, J. C.; Galgani, F.; Ryan, P. G.; Reisser, J. Plastic Pollution in the World's Oceans: More than 5 Trillion Plastic Pieces Weighing over 250,000 Tons Afloat at Sea. *PLoS One* **2014**, *9* (12), e111913.
- (7) Zhang, X.; Fevre, M.; Jones, G. O.; Waymouth, R. M. Catalysis as an Enabling Science for Sustainable Polymers. *Chem. Rev.* **2018**, 118 (2), 839–885.
- (8) Vroman, I.; Tighzert, L. Biodegradable Polymers. *Materials* **2009**, 2 (2), 307–344.

- (9) Nayak, P. L. Biodegradable Polymers: Opportunities and Challenges. J. Macromol. Sci., Polym. Rev. 1999, 39 (3), 481–505.
- (10) Galbis, J. A.; García-Martín, M. de G.; de Paz, M. V.; Galbis, E. Synthetic Polymers from Sugar-Based Monomers. *Chem. Rev.* **2016**, *116* (3), 1600–1636.
- (11) Guillaume, S. M.; Kirillov, E.; Sarazin, Y.; Carpentier, J.-F. Beyond Stereoselectivity, Switchable Catalysis: Some of the Last Frontier Challenges in Ring-Opening Polymerization of Cyclic Esters. *Chem. Eur. J.* **2015**, 21 (22), 7988–8003.
- (12) Panchal, S. S.; Vasava, D. V. Biodegradable Polymeric Materials: Synthetic Approach. ACS Omega 2020, 5 (9), 4370–4379.
- (13) Ashter, S. A. Introduction. In *Introduction to Bioplastics Engineering*; Ashter, S. A., Ed.; Plastics Design Library; Elsevier/William Andrew Publishing: Oxford, 2016; pp 1–17.
- (14) Wei, Y.; Wang, S.; Zhou, S. Aluminum Alkyl Complexes: Synthesis, Structure, and Application in ROP of Cyclic Esters. *Dalton Trans.* **2016**, *45* (11), 4471–4485.
- (15) Dechy-Cabaret, O.; Martin-Vaca, B.; Bourissou, D. Controlled Ring-Opening Polymerization of Lactide and Glycolide. *Chem. Rev.* **2004**, *104* (12), 6147–6176.
- (16) Wu, J.; Yu, T.-L.; Chen, C.-T.; Lin, C.-C. Recent Developments in Main Group Metal Complexes Catalyzed/Initiated Polymerization of Lactides and Related Cyclic Esters. *Coord. Chem. Rev.* **2006**, 250 (5), 602–626.
- (17) Jianming, R.; Anguo, X.; Hongwei, W.; Hailin, Y. Review Recent Development of Ring-Opening Polymerization of Cyclic Esters Using Aluminum Complexes. *Des. Monomers Polym.* **2014**, *17* (4), 345–355.
- (18) Gao, J.; Zhu, D.; Zhang, W.; Solan, G. A.; Ma, Y.; Sun, W.-H. Recent Progress in the Application of Group 1, 2 & 13 Metal Complexes as Catalysts for the Ring Opening Polymerization of Cyclic Esters. *Inorg. Chem. Front.* **2019**, *6* (10), 2619–2652.
- (19) Wang, Y.; Ma, H. Exploitation of Dinuclear Salan Aluminum Complexes for Versatile Copolymerization of ε -Caprolactone and L-Lactide. *Chem. Commun.* **2012**, 48 (53), 6729–6731.
- (20) Wang, Y.; Ma, H. Aluminum Complexes of Bidentate Phenoxy-Amine Ligands: Synthesis, Characterization and Catalysis in Ring-Opening Polymerization of Cyclic Esters. *J. Organomet. Chem.* **2013**, 731, 23–28.
- (21) Chen, L.; Li, W.; Yuan, D.; Zhang, Y.; Shen, Q.; Yao, Y. Syntheses of Mononuclear and Dinuclear Aluminum Complexes Stabilized by Phenolato Ligands and Their Applications in the Polymerization of ε -Caprolactone: A Comparative Study. *Inorg. Chem.* **2015**, 54 (10), 4699–4708.
- (22) Li, W.; Wu, W.; Wang, Y.; Yao, Y.; Zhang, Y.; Shen, Q. Bimetallic Aluminum Alkyl Complexes as Highly Active Initiators for the Polymerization of ε -Caprolactone. *Dalton Trans.* **2011**, *40* (43), 11378–11381.
- (23) Kaler, S.; McKeown, P.; Ward, B. D.; Jones, M. D. Aluminium(Iii) and Zinc(Ii) Complexes of Azobenzene-Containing Ligands for Ring-Opening Polymerisation of ε-Caprolactone and Rac-Lactide. *Inorg. Chem. Front.* **2021**, 8 (3), 711–719.
- (24) Yu, X.; Zhang, C.; Wang, Z. Controlled Polymerization of ϵ -Caprolactone Using Aluminum and Zinc Complexes with Iminophosphorane Ligands. *ChemistrySelect* **2020**, 5 (1), 426–429.
- (25) Diteepeng, N.; Wilson, I. A. P.; Buffet, J.-C.; Turner, Z. R.; O'Hare, D. L- and Rac-Lactide Polymerisation Using Scandium and Aluminium Permethylindenyl Complexes. *Polym. Chem.* **2020**, *11* (39), 6308–6318.
- (26) Campirán-Martínez, A.; Jancik, V.; Martínez-Otero, D.; Hernández-Balderas, U.; Zavala-Segovia, N.; Moya-Cabrera, M. Linkage Isomerism in Dinuclear Al and Ga Organometallic Complexes: Structural and Reactivity Consequences. *Organometallics* **2020**, *39* (10), 1799–1813.
- (27) Bouyahyi, M.; Roisnel, T.; Carpentier, J.-F. Aluminum Complexes of Bidentate Fluorinated Alkoxy-Imino Ligands: Syntheses, Structures, and Use in Ring-Opening Polymerization of Cyclic Esters. *Organometallics* **2012**, *31* (4), 1458–1466.

- (28) Wang, P.; Hao, X.; Cheng, J.; Chao, J.; Chen, X. Aluminum Chelates Supported by β -Quinolyl Enolate Ligands: Synthesis and ROP of ε -CL. Dalton Trans. **2016**, 45 (22), 9088–9096.
- (29) Zhang, Q.; Zhang, W.; Rajendran, N. M.; Liang, T.; Sun, W.-H. Thermo-Enhanced Ring-Opening Polymerization of ε -Caprolactone: The Synthesis, Characterization, and Catalytic Behavior of Aluminum Hydroquinolin-8-Olates. *Dalton Trans.* **2017**, 46 (24), 7833–7843.
- (30) Nakonkhet, C.; Nanok, T.; Wattanathana, W.; Chuawong, P.; Hormnirun, P. Aluminium Complexes Containing Salicylbenzothiazole Ligands and Their Application in the Ring-Opening Polymerisation of Rac-Lactide and ε -Caprolactone. *Dalton Trans.* **2017**, 46 (33), 11013–11030.
- (31) Sumrit, P.; Chuawong, P.; Nanok, T.; Duangthongyou, T.; Hormnirun, P. Aluminum Complexes Containing Salicylbenzoxazole Ligands and Their Application in the Ring-Opening Polymerization of Rac-Lactide and ε -Caprolactone. *Dalton Trans.* **2016**, 45 (22), 9250–9266.
- (32) Ma, W.-A.; Wang, Z.-X. Synthesis and Characterisation of Aluminium(Iii) and Tin(Ii) Complexes Bearing Quinoline-Based N,N,O-Tridentate Ligands and Their Catalysis in the Ring-Opening Polymerisation of ε -Caprolactone. *Dalton Trans.* **2011**, *40* (8), 1778–1786
- (33) Chuang, H.-J.; Su, Y.-C.; Ko, B.-T.; Lin, C.-C. Synthesis and Structural Characterization of Aluminum Complexes Supported by NNO-Tridentate Ketiminate Ligands: Efficient Catalysts for Ring-Opening Polymerization of l-Lactide. *Inorg. Chem. Commun.* **2012**, *18*, 38–42.
- (34) Sun, W.-H.; Shen, M.; Zhang, W.; Huang, W.; Liu, S.; Redshaw, C. Methylaluminium 8-Quinolinolates: Synthesis, Characterization and Use in Ring-Opening Polymerization (ROP) of ε -Caprolactone. *Dalton Trans.* **2011**, *40* (11), 2645–2653.
- (35) Chen, C.-T.; Huang, C.-A.; Huang, B.-H. Aluminium Metal Complexes Supported by Amine Bis-Phenolate Ligands as Catalysts for Ring-Opening Polymerization of ε -Caprolactone. *Dalton Trans.* **2003**, *19*, 3799–3803.
- (36) Hild, F.; Neehaul, N.; Bier, F.; Wirsum, M.; Gourlaouen, C.; Dagorne, S. Synthesis and Structural Characterization of Various N,O,N-Chelated Aluminum and Gallium Complexes for the Efficient ROP of Cyclic Esters and Carbonates: How Do Aluminum and Gallium Derivatives Compare? *Organometallics* **2013**, 32 (2), 587–598
- (37) Gao, B.; Li, X.; Duan, R.; Duan, Q.; Li, Y.; Pang, X.; Zhuang, H.; Chen, X. Hemi-Salen Aluminum Catalysts Bearing N, N, O-Tridentate Type Binaphthyl-Schiff-Base Ligands for the Living Ring-Opening Polymerisation of Lactide. *RSC Adv.* **2015**, *5* (37), 29412–29419.
- (38) Meduri, A.; Cozzolino, M.; Milione, S.; Press, K.; Sergeeva, E.; Tedesco, C.; Mazzeo, M.; Lamberti, M. Yttrium and Aluminium Complexes Bearing Dithiodiolate Ligands: Synthesis and Application in Cyclic Ester Polymerization. *Dalton Trans.* **2015**, *44* (41), 17990–18000.
- (39) Rajendran, N. M.; Xi, Y.; Zhang, W.; Braunstein, P.; Liang, T.; Sun, W.-H. Magnesium and Aluminum Complexes Bearing Bis(5,6,7-Trihydro Quinolyl)-Fused Benzodiazepines for ε -Caprolactone Polymerization. *Inorg. Chem. Front.* **2016**, 3 (10), 1317–1325.
- (40) Huang, W.-Y.; Chuang, S.-J.; Chunag, N.-T.; Hsiao, C.-S.; Datta, A.; Chen, S.-J.; Hu, C.-H.; Huang, J.-H.; Lee, T.-Y.; Lin, C.-H. Aluminium Complexes Containing Bidentate and Symmetrical Tridentate Pincer Type Pyrrolyl Ligands: Synthesis, Reactions and Ring Opening Polymerization. *Dalton Trans.* 2011, 40 (28), 7423–7433
- (41) Dagorne, S.; Le Bideau, F.; Welter, R.; Bellemin-Laponnaz, S.; Maisse-François, A. Well-Defined Cationic Alkyl— and Alkoxide—Aluminum Complexes and Their Reactivity with ε -Caprolactone and Lactides. *Chem. Eur. J.* **2007**, *13* (11), 3202–3217.
- (42) Fneich, B. N.; Das, A.; Kirschbaum, K.; Mason, M. R. Bidentate and Tridentate Coordination Modes of Bis(3-Methylindolyl)-2-Pyridylmethane in Complexes of Aluminum and Gallium: Structural

- Characterization of Bridging N-Indolide in a Dialuminum Complex. *J. Organomet. Chem.* **2018**, 872, 12–23.
- (43) Hair, G. S.; Battle, S. L.; Decken, A.; Cowley, A. H.; Jones, R. A. Synthesis and Characterization of 8-(Dimethylamino)-1-Naphthyl Derivatives of Aluminum, Gallium, and Indium. *Inorg. Chem.* **2000**, *39* (1), 27–31.
- (44) Zheng, W.; Roesky, H. W. Alkynyl Aluminium Compounds: Bonding Modes and Structures. *J. Chem. Soc., Dalton Trans.* **2002**, *14*, 2787–2796.
- (45) Huang, Y.-T.; Wang, W.-C.; Hsu, C.-P.; Lu, W.-Y.; Chuang, W.-J.; Chiang, M. Y.; Lai, Y.-C.; Chen, H.-Y. The Ring-Opening Polymerization of ε -Caprolactone and l-Lactide Using Aluminum Complexes Bearing Benzothiazole Ligands as Catalysts. *Polym. Chem.* **2016**, 7 (26), 4367–4377.
- (46) Nomura, N.; Ishii, R.; Akakura, M.; Aoi, K. Stereoselective Ring-Opening Polymerization of Racemic Lactide Using Aluminum-Achiral Ligand Complexes: Exploration of a Chain-End Control Mechanism. *J. Am. Chem. Soc.* **2002**, *124*, 5938–5939.
- (47) Du, H.; Pang, X.; Yu, H.; Zhuang, X.; Chen, X.; Cui, D.; Wang, X.; Jing, X. Polymerization of Rac-Lactide Using Schiff Base Aluminum Catalysts: Structure, Activity, and Stereoselectivity. *Macromolecules* **2007**, *40* (6), 1904–1913.
- (48) Tang, Z.; Chen, X.; Pang, X.; Yang, Y.; Zhang, X.; Jing, X. Stereoselective Polymerization of Rac-Lactide Using a Monoethylaluminum Schiff Base Complex. *Biomacromolecules* **2004**, 5 (3), 965–970.
- (49) Tang, Z.; Yang, Y.; Pang, X.; Hu, J.; Chen, X.; Hu, N.; Jing, X. Controlled and Stereospecific Polymerization of Rac-Lactide with a Single-Site Ethyl Aluminum and Alcohol Initiating System. *J. Appl. Polym. Sci.* **2005**, 98 (1), 102–108.
- (50) Nomura, N.; Ishii, R.; Yamamoto, Y.; Kondo, T. Stereoselective Ring-Opening Polymerization of a Racemic Lactide by Using Achiral Salen—and Homosalen—Aluminum Complexes. *Chem. Eur. J.* **2007**, 13 (16), 4433—4451.
- (51) Bolley, A.; Mameri, S.; Dagorne, S. Controlled and Highly Effective Ring-Opening Polymerization of α -Chloro- ε -Caprolactone Using Zn- and Al-Based Catalysts. *J. Polym. Sci.* **2020**, *58* (9), 1197–1206.
- (52) Hormnirun, P.; Marshall, E. L.; Gibson, V. C.; White, A. J. P.; Williams, D. J. Remarkable Stereocontrol in the Polymerization of Racemic Lactide Using Aluminum Initiators Supported by Tetradentate Aminophenoxide Ligands. *J. Am. Chem. Soc.* **2004**, *126* (9), 2688–2689.
- (53) Du, H.; Velders, A. H.; Dijkstra, P. J.; Sun, J.; Zhong, Z.; Chen, X.; Feijen, J. Chiral Salan Aluminium Ethyl Complexes and Their Application in Lactide Polymerization. *Chem. Eur. J.* **2009**, *15* (38), 9836–9845.
- (54) Press, K.; Goldberg, I.; Kol, M. Mechanistic Insight into the Stereochemical Control of Lactide Polymerization by Salan–Aluminum Catalysts. *Angew. Chem., Int. Ed.* **2015**, 54 (49), 14858–14861.
- (55) Trofimenko, S. Boron-Pyrazole Chemistry. J. Am. Chem. Soc. 1966, 88 (8), 1842–1844.
- (56) Trofimenko, S. Transition Metal Poly(1-Pyrazolyl)Borates Containing Other Ligands. J. Am. Chem. Soc. 1967, 89 (15), 3904—3905
- (57) Trofimenko, S. Coordination Chemistry of Pyrazole-Derived Ligands. *Chem. Rev.* **1972**, 72 (5), 497–509.
- (58) Owen, G. R. Functional Group Migrations between Boron and Metal Centres within Transition Metal-Borane and Boryl Complexes and Cleavage of H–H, E–H and E–E' Bonds. *Chem. Commun.* **2016**, 52 (71), 10712–10726.
- (59) Pettinari, C.; Pettinari, R.; Marchetti, F. Golden Jubilee for Scorpionates: Recent Advances in Organometallic Chemistry and Their Role in Catalysis. In *Advances in Organometallic Chemistry*, Vol. 65; Pérez, P. J., Ed.; Academic Press, 2016; Chapter 4, pp 175–260.
- (60) Wang, Y.; Zhang, B.; Guo, S. Transition Metal Complexes Supported by N-Heterocyclic Carbene-Based Pincer Platforms:

- Synthesis, Reactivity and Applications. Eur. J. Inorg. Chem. 2021, 2021 (3), 188–204.
- (61) Taakili, R.; Canac, Y. NHC Core Pincer Ligands Exhibiting Two Anionic Coordinating Extremities. *Molecules* **2020**, 25 (9), 2231.
- (62) Silva, F.; Fernandes, C.; Campello, M. P. C.; Paulo, A. Metal Complexes of Tridentate Tripod Ligands in Medical Imaging and Therapy. *Polyhedron* **2017**, *125*, 186–205.
- (63) Martins, L. M. D. R. S. C-Scorpionate Complexes: Ever Young Catalytic Tools. *Coord. Chem. Rev.* **2019**, 396, 89–102.
- (64) Santini, C.; Marinelli, M.; Pellei, M. Boron-Centered Scorpionate-Type NHC-Based Ligands and Their Metal Complexes. *Eur. J. Inorg. Chem.* **2016**, 2016 (15–16), 2312–2331.
- (65) Otero, A.; Fernández-Baeza, J.; Antiñolo, A.; Tejeda, J.; Lara-Sánchez, A. Heteroscorpionate Ligands Based on Bis(Pyrazol-1-Yl)Methane: Design and Coordination Chemistry. *Dalton Trans.* **2004**, *10*, 1499–1510.
- (66) de la Cruz-Martínez, F.; Martínez, J.; Gaona, M. A.; Fernández-Baeza, J.; Sánchez-Barba, L. F.; Rodríguez, A. M.; Castro-Osma, J. A.; Otero, A.; Lara-Sánchez, A. Bifunctional Aluminum Catalysts for the Chemical Fixation of Carbon Dioxide into Cyclic Carbonates. *ACS Sustainable Chem. Eng.* **2018**, *6* (4), 5322–5332.
- (67) Garcés, A.; Sánchez-Barba, L. F.; Fernández-Baeza, J.; Otero, A.; Fernández, I.; Lara-Sánchez, A.; Rodríguez, A. M. Organo-Aluminum and Zinc Acetamidinates: Preparation, Coordination Ability, and Ring-Opening Polymerization Processes of Cyclic Esters. *Inorg. Chem.* **2018**, 57 (19), 12132–12142.
- (68) Su, W.-J.; Liang, L.-C. Elusive Scorpionates: C3-Symmetric, Formally Dianionic, Facially Tridentate Ligands. *Inorg. Chem.* **2018**, 57 (2), 553–556.
- (69) Martínez, J.; Castro-Osma, J. A.; Alonso-Moreno, C.; Rodríguez-Diéguez, A.; North, M.; Otero, A.; Lara-Sánchez, A. One-Component Aluminum(Heteroscorpionate) Catalysts for the Formation of Cyclic Carbonates from Epoxides and Carbon Dioxide. *ChemSusChem* **2017**, *10* (6), 1175–1185.
- (70) Martínez, J.; Castro-Osma, J. A.; Earlam, A.; Alonso-Moreno, C.; Otero, A.; Lara-Sánchez, A.; North, M.; Rodríguez-Diéguez, A. Synthesis of Cyclic Carbonates Catalysed by Aluminium Heteroscorpionate Complexes. *Chem. Eur. J.* **2015**, *21* (27), 9850–9862.
- (71) Chen, H.-Y.; Lee, Y.-H.; Chiang, M. Y.; Lu, W.-Y.; Tseng, H.-C.; Tsai, H.-Y.; Chen, Y.-H.; Lai, Y.-C.; Chen, H.-Y. Coordinating Effect in Ring-Opening Polymerization of ε -Caprolactone Using Aluminum Complexes Bearing Bisphenolate as Catalysts. *RSC Adv.* **2015**, 5 (100), 82018-82026.
- (72) Castro-Osma, J. A.; Alonso-Moreno, C.; Márquez-Segovia, I.; Otero, A.; Lara-Sánchez, A.; Fernández-Baeza, J.; Rodríguez, A. M.; Sánchez-Barba, L. F.; García-Martínez, J. C. Synthesis, Structural Characterization and Catalytic Evaluation of the Ring-Opening Polymerization of Discrete Five-Coordinate Alkyl Aluminium Complexes. *Dalton Trans.* **2013**, *42* (25), 9325–9337.
- (73) Otero, A.; Lara-Sánchez, A.; Fernández-Baeza, J.; Alonso-Moreno, C.; Castro-Osma, J. A.; Márquez-Segovia, I.; Sánchez-Barba, L. F.; Rodríguez, A. M.; Garcia-Martinez, J. C. Neutral and Cationic Aluminum Complexes Supported by Acetamidate and Thioacetamidate Heteroscorpionate Ligands as Initiators for Ring-Opening Polymerization of Cyclic Esters. *Organometallics* **2011**, 30 (6), 1507–1522.
- (74) Castro-Osma, J. A.; Alonso-Moreno, C.; Lara-Sanchez, A.; Otero, A.; Fernandez-Baeza, J.; Sanchez-Barba, L. F.; Rodriguez, A. M. Catalytic Behaviour in the Ring-Opening Polymerisation of Organo-aluminiums Supported by Bulky Heteroscorpionate Ligands. *Dalton Trans.* 2015, 44 (27), 12388–12400.
- (75) Castro-Osma, J. A.; Alonso-Moreno, C.; García-Martinez, J. C.; Fernández-Baeza, J.; Sánchez-Barba, L. F.; Lara-Sánchez, A.; Otero, A. Ring-Opening (ROP) versus Ring-Expansion (REP) Polymerization of ε -Caprolactone To Give Linear or Cyclic Polycaprolactones. *Macromolecules* **2013**, *46* (16), 6388–6394.
- (76) Gazizov, A. S.; Burilov, A. R.; Khakimov, M. S.; Kharitonova, N. I.; Pudovik, M. A.; Konovalov, A. I. Reaction of α -Aminoacetals with 2-Methylresorcinol. *Russ. J. Gen. Chem.* **2009**, 79 (9), 1929–1930.

- (77) Aoyama, K. Latent Epoxy Curing Catalyst or Curing Agent. WO 2018181045, 2018.
- (78) Yu, R.-C.; Hung, C.-H.; Huang, J.-H.; Lee, H.-Y.; Chen, J.-T. Four- and Five-Coordinate Aluminum Ketiminate Complexes: Synthesis, Characterization, and Ring-Opening Polymerization. *Inorg. Chem.* **2002**, *41* (24), 6450–6455.
- (79) Silvestri, A.; Grisi, F.; Milione, S. Ring Opening Polymerization of Lactide Promoted by Alcoholyzed Heteroscorpionate Aluminum Complexes. J. Polym. Sci., Part A: Polym. Chem. 2010, 48 (16), 3632–3639
- (80) Arbaoui, A.; Redshaw, C. Metal Catalysts for ε -Caprolactone Polymerisation. *Polym. Chem.* **2010**, *1* (6), 801–826.
- (81) Huang, T.-W.; Su, R.-R.; Lin, Y.-C.; Lai, H.-Y.; Yang, C.-Y.; Senadi, G. C.; Lai, Y.-C.; Chiang, M. Y.; Chen, H.-Y. Improvement in Aluminum Complexes Bearing a Schiff Base in Ring-Opening Polymerization of ε -Caprolactone: The Synergy of the N,S-Schiff Base in a Five-Membered Ring Aluminum System. *Dalton Trans.* **2018**, 47 (43), 15565–15573.
- (82) Lu, W.-Y.; Chang, Y.-C.; Lian, C.-J.; Wu, K.-H.; Chiang, M. Y.; Chen, H.-Y.; Lin, C.-C.; Ko, B.-T. Optimization of Six-Membered Ring Aluminum Complexes in ε -Caprolactone Polymerization. *Eur. Polym. J.* **2019**, *114*, 151–163.